

NASA CR 54818  
AGC 8800-16



N66-17 285

FACILITY FORM 802

|                               |            |
|-------------------------------|------------|
| (ACCESSION NUMBER)            | (THRU)     |
| 85                            | 1          |
| (PAGES)                       | (CODE)     |
| CR-54818                      | 15         |
| (NASA CR OR TMX OR AD NUMBER) | (CATEGORY) |

DEVELOPMENT OF LARGE SIZE BELLOWS  
FACE TYPE SEALS FOR LIQUID OXYGEN AND OXYGEN/HYDROGEN  
HOT GAS SERVICE AT MODERATE TO HIGH PRESSURES

GPO PRICE \$ \_\_\_\_\_

By

CFSTI PRICE(S) \$ \_\_\_\_\_

E. Roesch  
T. Pasternak

Hard copy (HC) 3.00

Microfiche (MF) .75

ff 853 July 85

Prepared for  
National Aeronautics and Space Administration

Contract NAS 3-2555



AEROJET-GENERAL CORPORATION

SACRAMENTO, CALIFORNIA

## NOTICE

This report was prepared as an account of Government sponsored work. Neither the United States, nor the National Aeronautics and Space Administration (NASA), nor any person acting on behalf of NASA:

- A.) Makes any warranty or representation, expressed or implied, with respect to the accuracy, completeness, or usefulness of the information contained in this report, or that the use of any information, apparatus, method or process disclosed in this report may not infringe privately owned rights, or
- B.) Assumes any liabilities with respect to the use of, or for damages resulting from the use of any information, apparatus, method or process disclosed in this report.

As used above, "person acting on behalf of NASA" includes any employee or contractor of NASA, or employee of such contractor, to the extent that such employee or contractor of NASA, or employee of such contractor prepares, disseminates, or provides access to, any information pursuant to his employment or contract with NASA, or his employment with such contractor.

Requests for copies of this report should be referred to:

National Aeronautics and Space Administration  
Office of Scientific and Technical Information  
Attention: AFSS-A  
Washington, D. C. 20546

TECHNOLOGY REPORT

DEVELOPMENT OF LARGE SIZE BELLOWS FACE TYPE SEALS  
FOR  
LIQUID OXYGEN AND OXYGEN/HYDROGEN HOT GAS SERVICE  
AT MODERATE TO HIGH PRESSURES

Prepared for

National Aeronautics and Space Administration

10 February 1966

Contract NAS3-2555

Prepared by:

Aerojet-General Corporation  
Liquid Rocket Operations  
Sacramento, California

Technical Management:

NASA Lewis Research Center  
Cleveland, Ohio

Authors: E. Roesch and T. Pasternak

Technical Manager: K. L. Baskin

Approved:

W. E. Campbell  
Manager  
M-1 Turbopump Project

Approved:

W. F. Dankhoff  
M-1 Project Manager



# ABSTRACT

17285  
This report describes the development program wherein a four-element dynamic face seal was evaluated for an application requiring positive separation of cryogenic bearing coolant and hot gas in a turbopump. The objective was accomplished by separating the media via a neutral gaseous nitrogen purge. This system was applied to the M-1 turbopump and performed successfully.

Initially, it was attempted to develop the seal leakage control without having to rely on a buffer gas. This effort was discontinued when it became apparant that extrapolation of conventional and small size seal technology did not produce the required minimum leakage performance for this critical application.

The solution of using a buffer gas provided an expediency to allow proceeding with turbopump and engine development. (in this)



## TABLE OF CONTENTS

|   | <u>PAGE</u> |
|---|-------------|
| I. <u>SUMMARY</u>   | 1           |
| II. <u>INTRODUCTION</u>                                       | 2           |
| III. <u>SEAL DEVELOPMENT PROGRAM</u>                          | 2           |
| A. PROGRAM OBJECTIVES   | 2           |
| 1. <u>Seal Application in the M-1 Liquid Oxygen Turbopump</u> | 2           |
| 2. <u>Unusual Requirements</u>                                | 4           |
| B. DESIGN SELECTION   | 4           |
| 1. <u>Design Criteria</u>                                     | 4           |
| 2. <u>Seal Selection and Alternative Solutions</u>            | 5           |
| 3. <u>Sealol Seal</u>   | 6           |
| 4. <u>Borg Warner Seal</u>                                    | 6           |
| C. SEAL DEVELOPMENT TESTING                                   | 6           |
| 1. <u>Scope of Test Activity</u>                              | 6           |
| a. Face Material Evaluation                                   | 6           |
| (1) Test Equipment  | 6           |
| (2) Test Development Activity                                 | 13          |
| (3) Test Development Results                                  | 13          |
| b. Full-Scale Seal Testing                                    | 17          |
| (1) Test Equipment  | 17          |
| (2) Test Development Activity                                 | 22          |
| (3) Test Development Results                                  | 22          |

## TABLE OF CONTENTS (cont.)

|  | <u>PAGE</u> |
|--|-------------|
| c.    Effective Diameter Test Measurements   | 29          |
| (1) Terminology  | 29          |
| (2) Measurement System   | 30          |
| (3) Equipment  | 31          |
| (4) Test Activity and Results  | 37          |
| 2. <u>Test Activity Conclusions</u>  | 37          |
| D.    MODIFICATION OF THE SEAL SYSTEM FOR TURBOPUMP USE                                | 42          |
| 1. <u>Concept and Design Philosophy</u>  | 42          |
| 2. <u>Seal Hardware Modification</u>   | 42          |
| E.    APPLICATION OF THE MODIFIED SEAL SYSTEM IN THE M-1<br>MODEL I OXIDIZER TURBOPUMP | 44          |
| 1. <u>Installation of Modified Seal System</u>   | 44          |
| 2. <u>Performance During Turbopump Testing</u>   | 44          |
| IV. <u>CONCLUSIONS AND RECOMMENDATIONS</u>   | 50          |
| BIBLIOGRAPHY   |             |
| APPENDICES   |             |
| A.    NOMENCLATURE   |             |
| B.    ANALYTICAL TREATMENT OF SEAL LEAKAGE   |             |

## LIST OF TABLES

| <u>TABLE NO.</u> | <u>TITLE</u>   | <u>PAGE</u> |
|------------------|--|-------------|
| 1                | Summary of Seal Material Evaluation Tests for Liquid Oxygen Seal in Subscale Seal Tester | 15          |
| 2                | Summary of Seal Material Evaluation Tests for Hot Gas Seal in Subscale Seal Tester       | 16          |
| 3                | Summary of Prototype Seal Tests  | 24          |

## LIST OF FIGURES

| <u>FIGURE NO.</u> | <u>TITLE</u>   | <u>PAGE</u> |
|-------------------|--|-------------|
| 1                 | Seal Location in the M-1 Liquid Oxygen Turbopump       | 3           |
| 2                 | Sealol Seal Assembly                                   | 7           |
| 3                 | Oxidizer Turbine Seal Assembly, AGC Drawing No. 280115 | 8           |
| 4                 | Borg Warner Seal Assembly                              | 9           |
| 5                 | Oxidizer Turbine Seal Assembly, AGC Drawing No. 284938 | 10          |
| 6                 | Subscale Seal Test Fixture, AGC Drawing No. 261760     | 11          |
| 7                 | Subscale Seal Test Facility                            | 14          |
| 8                 | Full Scale Seal Test Facility                          | 18          |
| 9                 | Full Scale Seal Tester, AGC Drawing No. 291472         | 19          |
| 10                | Typical Prototype Seal                                 | 23          |
| 11                | Lapped Seal Face-Talysurf Surface Measurement          | 26          |
| 12                | Lapped Seal Face-Talyrond Surface Measurement          | 27          |
| 13                | Typical Effective Diameter Seal Test Fixture           | 32          |
| 14                | Effective Diameter Tester, AGC Drawing No. 291482      | 33          |
| 15                | Effective Diameter Tester, AGC Drawing No. 291530      | 35          |

LIST OF FIGURES (cont.)

| <u>FIGURE NO.</u> | <u>TITLE</u>  | <u>PAGE</u> |
|-------------------|---|-------------|
| 16                | Effective Diameter vs Ext. Pressure, 0.093 Compression  | 38          |
| 17                | Effective Diameter vs Ext. Pressure, 0.123 Compression  | 39          |
| 18                | Over Balance vs External Pressure, 0.093 Compression    | 40          |
| 19                | Over Balance vs External Pressure, 0.123 Compression    | 41          |
| 20                | Modified Seal System Schematic                          | 43          |
| 21                | Seal Assembly, Oxidizer Turbine, AGC Drawing No. 700794 | 45          |
| 22                | Modified Seal System, - Oxygen Drain                    | 47          |
| 23                | Modified Seal System, - Hot Gas Drain                   | 48          |
| 24                | Modified Seal System, - Gaseous Nitrogen Purge Supply   | 49          |

## I. SUMMARY

The activity and results of the program to develop the turbine-end dynamic sealing system for the M-1 engine oxidizer turbopump assembly are described.

The fluids to be separated are liquid oxygen at a pressure of 550 psia and a gas consisting of a mixture of hydrogen and steam at a temperature of 900°F and a pressure of 125 psia. Shaft size and speed dictate a seal face rubbing velocity of about 120 ft/sec.

The conventional principle of a rubbing contact mechanical face seal was selected as the seal concept to be pursued. Within this scope, various design alternatives were considered and seal vendor capabilities investigated. The primary candidate was the Sealol seal, a design that utilizes a primary and a secondary seal face for liquid oxygen as well as for hot gas sealing. Also, a Borg Warner seal with a modified design was investigated.

Leakage control was recognized as the principle problem and the following development goal was established for allowable dynamic leakage:

|                                 |  |
|---------------------------------|--|
| Liquid Oxygen Seal - Primary:   | 30,000 Standard cc/min (1.06 SCFM)                 |
| Liquid Oxygen Seal - Secondary: | 100 Standard cc/min ( $3.531 \times 10^{-3}$ SCFM) |
| Hot Gas Seal - Primary:         | 3,000 Standard cc/min (0.106 SCFM)                 |
| Hot Gas Seal - Secondary:       | 10 Standard cc/min ( $3.531 \times 10^{-4}$ SCFM)  |

Generally, it appears that performance of a rubbing contact dynamic face seal, in terms of wear and minimum leakage, is strongly influenced by face material compatibility and load balance of the seal face. To develop optimum qualities for the subject seal, the full scale test effort was supplemented in two ways. A seal face material evaluation program was conducted on a subscale level and the effective diameter of the seal bellows was determined through the use of measurement techniques.

Full scale prototype tests were used to investigate possible leakage causes (i.e., vibration that could cause oscillatory separation of the seal faces; carbon nosepiece distortion caused by thermal and mechanical stress; pressure variation and gap effects caused by boiling of liquid oxygen across the seal face; incorrect face loading; and seal face flatness). As development continued, leakage control was somewhat improved, but still exceeded requirements. Typical leakages were as much as 800,000 scc/min (28.25 SCFM) across the liquid oxygen primary seal and 60,000 scc/min (2.12 SCFM) across the hot gas primary seal.

In evaluating the degree of performance accomplished through development, it was evident that significant further improvement would be needed to achieve either the established goal or to obtain the minimum performance necessary for turbopump operation. Timely accomplishment of this by further development of the same basic concept was considered impractical. Accordingly, the seal system was modified. This modification provided an inert (gaseous nitrogen) gas purge into the neutral cavity to supply both a secondary seal back pressure and a "washing" action to carry any primary leakage out through the respective cavity drains.

The technique of purging the "neutral" seal cavity provided the necessary seal effectiveness to prevent the mixing of fluids being separated. This modification of the seal system was installed into the M-1 Model I Liquid Oxygen Turbopump and it was successfully utilized and operated without failure during turbopump testing. However, the cryogenic bearing coolant for this test series was liquid nitrogen and not liquid oxygen.

## II. INTRODUCTION

The large size dynamic seal for liquid oxygen and oxygen/hydrogen hot gas service, was developed by the Aerojet-General Corporation under contract to the National Aeronautics and Space Administration. This seal development was for the specific application in the M-1 Engine Liquid Oxygen Turbopump.

In this turbopump the power transmission components are located between a centrifugal cryogenic propellant pump and a hot gas impulse turbine. A common shaft provides the transmission of driving power from the turbine rotor to the pump impeller. Bearings are cooled by the liquid oxygen supplied from the pump discharge and circulated through the power transmission housing. The cryogenic fluid in the bearing housing is kept at a relatively high pressure (550 psia) to maintain a satisfactory vapor pressure margin in the bearing coolant circuit. It was felt that for bearing coolant effectiveness, the liquid phase must be maintained in the fluid. To avoid the hazard of an explosion which could result from mixing of the hydrogen-rich turbine gas with the liquid oxygen bearing coolant, a reliable seal for separation of the fluid media is essential. Mechanically, it is necessary that the axial length of this seal assembly is kept to a minimum to keep the overhang of the turbine rotor within practical limits and maintain a safe critical speed value.

The development effort of this seal, which is located at the turbine interface of the M-1 turbopump, is the subject of this report.

## III. SEAL DEVELOPMENT PROGRAM

### A. PROGRAM OBJECTIVES

#### 1. Seal Application in the M-1 Liquid Oxygen Turbopump

The location of the subject seal assembly in the M-1 Liquid Oxygen Turbopump is shown by Figure 1. The purpose of this seal is to separate the liquid oxygen in the bearing housing from the hydrogen-rich hot turbine gas in the adjoining turbine cavity. Because the mixing of these fluids has the potentiality for an explosion, the effectiveness of the seal assembly is of vital importance for dependable turbopump operation and affects the over-all system design as to whether the pump can be wet or dry during coast periods prior to engine operation. This highly sensitive operating environment establishes the desirability of "Zero Leakage" seal performance.



Figure 1  
Oxidizer Turbopump - Seal Location  
Page 3

## 2. Unusual Requirements

Attainment of a true "zero leakage" seal performance is desirable but in view of the current technology status, it is generally considered an impossibility with rotating dynamic seals. For the specific application an interim goal was established permitting some mixing of liquid oxygen with hot gas at a maximum permissible rate of 100 scc/min liquid oxygen and 10 scc/min hot gas under dynamic operating conditions. Maximum allowable dynamic leakage past the primary LOX seal faces is 30,000 scc/min for the LOX seal and 3,000 scc/min for the hot gas seal. Maximum static leakage of liquid oxygen into the turbine cavity was established at 10 scc/min. This performance was to be obtained through development improvements by June 1966.

The volume ratio of oxygen gas at standard atmospheric pressure and temperature versus liquid oxygen is approximately 800/1. This means that a maximum allowable dynamic leakage of 100 standard cubic centimeters per minute (scc/min) is only  $100/800 = 0.12$  cc/min of liquid oxygen. This is an extremely low leakage requirement for a dynamic seal, particularly for one of the large proportions required for the 4 in. shaft diameter of the turbopump.

Seal face surface finish and flatness contribute significantly to seal performance for a rubbing contact seal. However, these qualities become more difficult to control with the relatively large diameter seal faces needed in this application. Dimensional stability is unfavorably influenced by the extreme axial and radial temperature gradients across the seal assembly separating the hot gas cavity on one side and the cryogenic fluid cooled bearing housing on the other. Heat generation resulting from dynamic friction is a further cause of thermal stress and associated seal face distortion. It appeared that optimum matching of seal face materials would be a decisive influence in achieving the leakage goal with a rubbing contact seal.

### B. DESIGN SELECTION

#### 1. Design Criteria

The primary requirement for this seal is to prevent mixing of the liquid oxygen with the hot turbine gas. Specific requirements include:

##### a. Maximum Allowable Dynamic Leakage Rates

|                                 |                        |
|---------------------------------|------------------------|
| Liquid Oxygen Seal - Primary:   | 30,000 Standard cc/min |
| Liquid Oxygen Seal - Secondary: | 100 Standard cc/min    |
| Hot Gas Seal - Primary:         | 3,000 Standard cc/min  |
| Hot Gas Seal - Secondary:       | 10 Standard cc/min     |

b. Dynamic Operating Conditions

|                                      |  |
|--------------------------------------|--|
| Shaft Speed                          | 4,000 rpm, Maximum   |
| Shaft Acceleration Rate<br>(Startup) | 120 Revolutions per<br>Sec <sup>2</sup> , Maximum                    |
| Allowable Shaft Runout<br>(Radial)   | 0.007-In.  |
| Shaft Axial Play                     | 0.018 to 0.023-In.   |
| Fluid Temperature                    |  |
| Liquid Oxygen Side                   | Minus 297°F  |
| Hot Gas Side                         | 917°F, Maximum   |
| Fluid Pressure                       |  |
| Liquid Oxygen Side                   | 550 psia   |
| Hot Gas Side                         | 125 psia   |
| Operating Medium                     |  |
| Pump Side                            | Liquid Oxygen  |
| Turbine Side                         | Turbine Gas (90% H <sub>2</sub> +<br>10% H <sub>2</sub> O by Volume) |
| Number of Starts                     | 30   |
| Life                                 | 10 Hours   |

c. Static Turbopump Operating Conditions

|   |                         |
|---|-------------------------|
| Maximum Pressure at<br>Liquid Oxygen Side | 65 psia for<br>12 hours |
| Minimum Pressure at<br>Hot Gas Side       | 0 psia                  |

2. Seal Selection and Alternative Solutions

The conventional principle of a rubbing contact mechanical seal was selected as the seal concept to be pursued during development. Within this scope, consideration was given to several arrangements of axial face seals, shaft riding seals, and a combination thereof. The concept of using two face seals in series for liquid oxygen and another two face seals in series for hot gas was selected based upon the results of this study. This concept included incorporation of a vent between each pair of seal faces to permit bleed-off of leakage from the primary liquid oxygen and primary hot gas seals. Liquid oxygen and hot gas leakage past the respective secondary seals is evacuated through a common "neutral" vent.

Several seal manufacturing firms, including Sealol, Gits Bros, Borg-Warner, and Chicago Rawhide were consulted regarding their experience and seal manufacturing capability. The Sealol Corporation of Providence, Rhode Island, was selected as the primary subcontractor because they indicated they were capable of manufacturing a seal for this application.

### 3. Sealol Seal

This seal assembly consists of primary and secondary seals on both the liquid oxygen and the hot gas side. Each of the four seal units is a bellows type, axial, mechanical face seal. The seal nosepieces are carbon rings bonded to their respective retainers. Each pair of seal faces contacts a common rotating ring. There are two rotating rings, one for the sealing of liquid oxygen and one for hot gas. The seal faces are held in contact with the respective rotating rings by the spring force of the bellows and the hydraulic pressure of the fluid being sealed. Any fluid which passes through the primary seals is vented to the atmosphere by separate lines for liquid oxygen and turbine gas, thus providing low upstream pressure on the secondary seals. Leakage through the secondary liquid oxygen and hot gas seals is vented through a common line. A general illustration of the seal is shown in Figures 2 and 3. The average rubbing velocity for this seal configuration is approximately 115 ft/sec.

### 4. Borg-Warner Seal

This seal assembly, Figures 4 and 5, was developed as an alternative design. It consists of three face seals, arranged axially in series. The two outer seals are the primary liquid oxygen seal and the primary hot gas seal, respectively. The assembly is designed so that any leakage from the primary liquid oxygen seal or from the primary hot gas seal will be segregated from each other by an intermediate seal. Any leakage from either of the two outer seals is vented separately to atmosphere. There are floating carbon rings between the stationary seal faces and the rotating rings. These floating carbon rings are intended to eliminate the effect of thermal deformations normally developed in retainers. Each seal has metal bellows and the arrangement provides for separate rotating rings spaced on the shaft by sleeve spacers. Rubbing velocity for this seal geometry is approximately 95 ft/sec.

## C. SEAL DEVELOPMENT TESTING

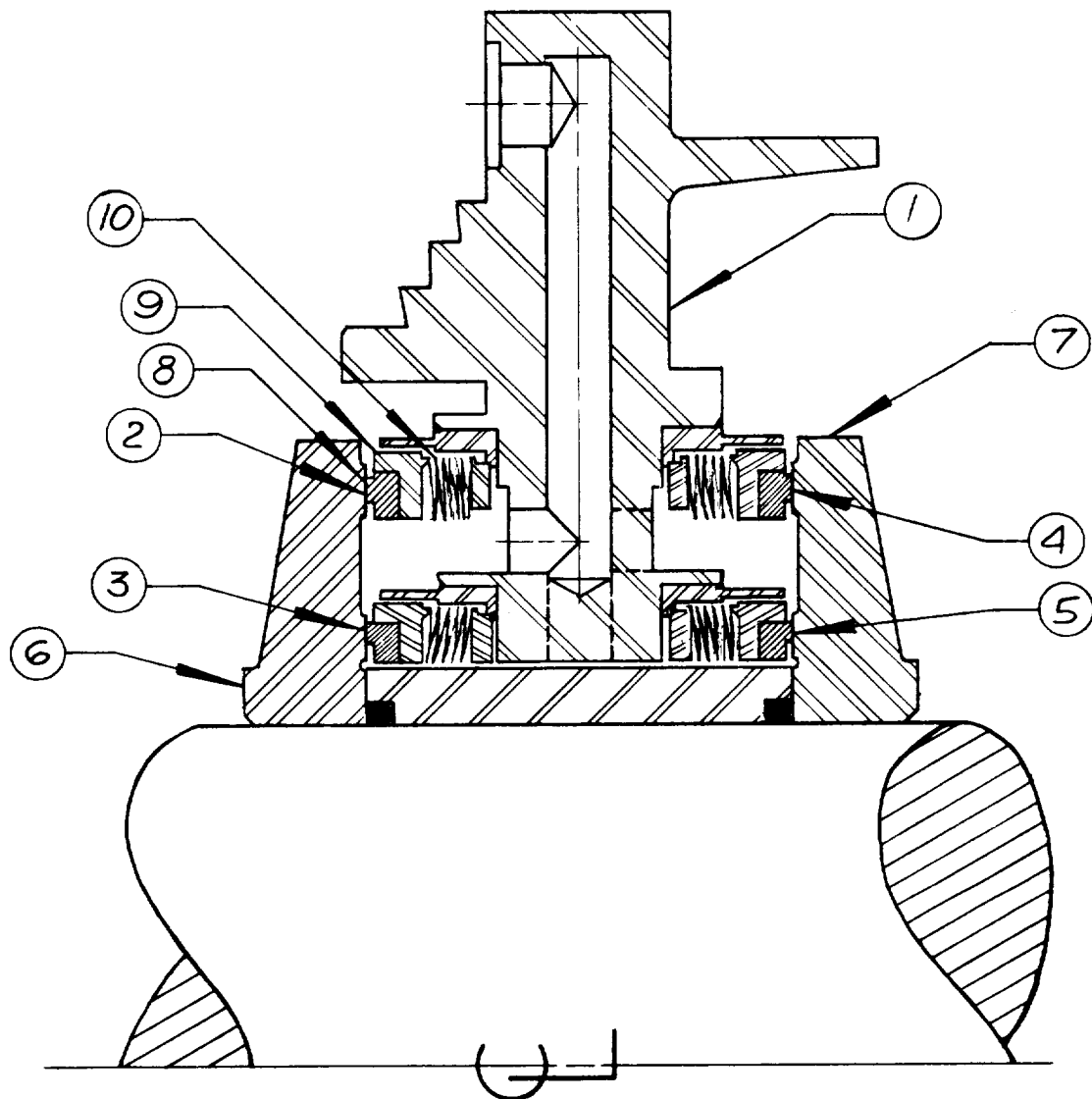
### 1. Scope of Test Activity

#### a. Face Material Evaluation

##### (1) Test Equipment

An evaluation program for candidate liquid oxygen and hot gas seal face materials was initiated concurrently with the design and manufacturing activity for the prototype seal configuration. This evaluation program was conducted with subscale (5/8 full size) seal assemblies because these seals were available and the existing tester configurations were adaptable. The tester, which is shown on Figure 6, consists of a drive unit and the test head. The drive unit is made up of a 27 HP air motor connected to a Titan I gearbox and the test

# SEALOL SEAL ASSEMBLY

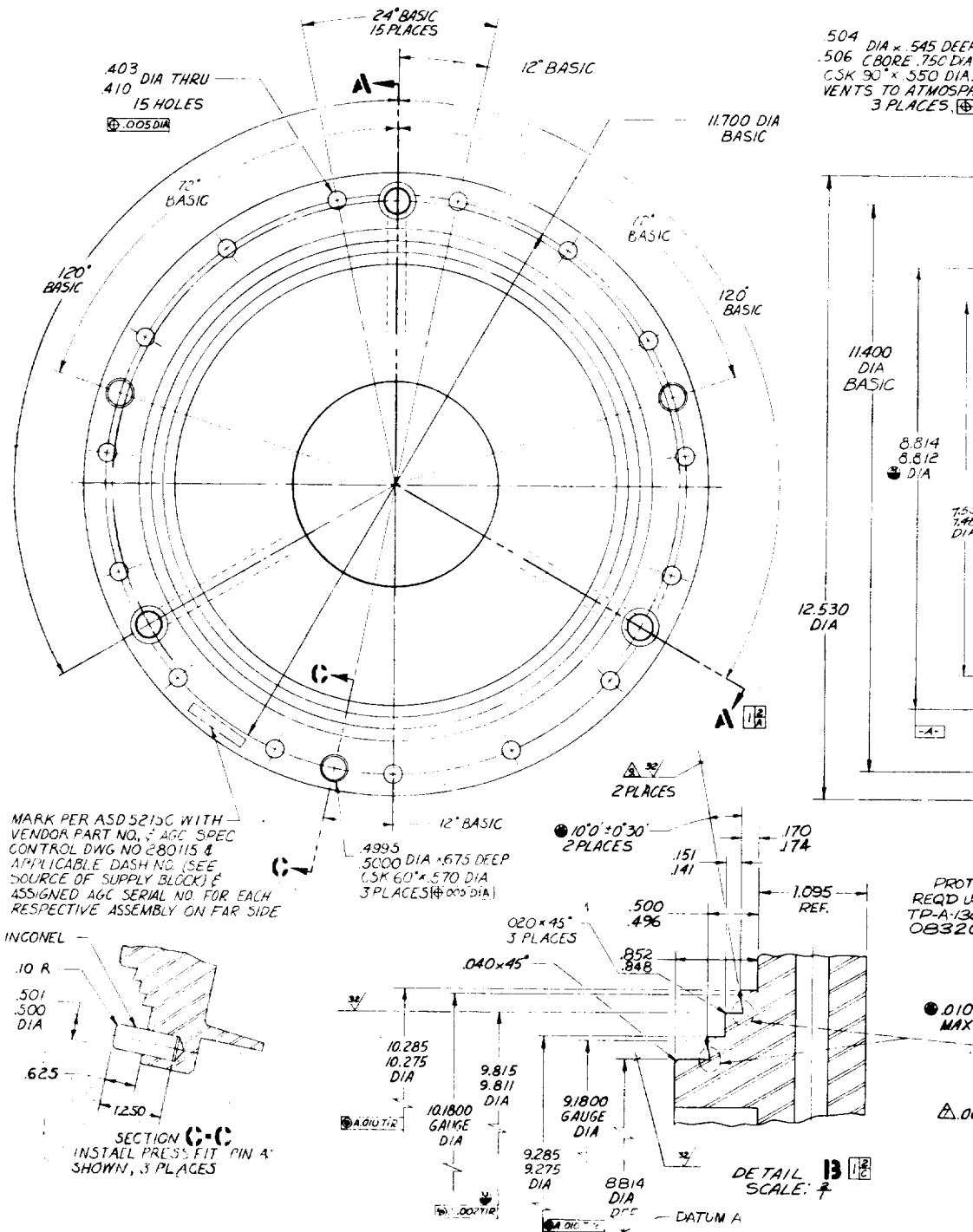


- |                             |                                 |
|-----------------------------|---------------------------------|
| 1. SEAL FLANGE              | 6. ROTATING RING - LOX          |
| 2. PRIMARY SEAL - LOX       | 7. ROTATING RING - HOT GAS      |
| 3. SECONDARY SEAL - LOX     | 8. CARBON NOSEPIECE - TYPICAL   |
| 4. PRIMARY SEAL - HOT GAS   | 9. NOSEPIECE RETAINER - TYPICAL |
| 5. SECONDARY SEAL - HOT GAS | 10. BELLOWS - TYPICAL           |

Figure 2



5. SEAL DEFINITION OF "MANUFACTURED" WILL BE DETERMINED BY THE TYPICAL AND UNUSUAL THINNESS.
6. ALL WELDS ARE TO BE FRS W/UTS.
7. ALL PERMITS ARE 16357, LESS 18. EXCEPTIVE & PACKAGE PERMITS, FUSelage COMPONENT.
8. THE VENDOR IS TO INDICATE ON ALL MATERIALS OF ALL COMPONENTS, THE DESIGN STATIC FACTOR, THE DESIGN STRESS, RATE, & COMPRESSED HEIGHT OF EACH THE DESIGN OVERBALANCE OF EACH SUB ASSY. AS APPLICABLE.
9. THE VENDOR SHALL SUPPLY MATERIAL DELIVERED TO THE BELLS, RATES, FREE LENGTH, & EFF. CURVES FROM ACTUAL TEST EACH SEAL SUBASSY.









# BORG WARNER SEAL ASSEMBLY

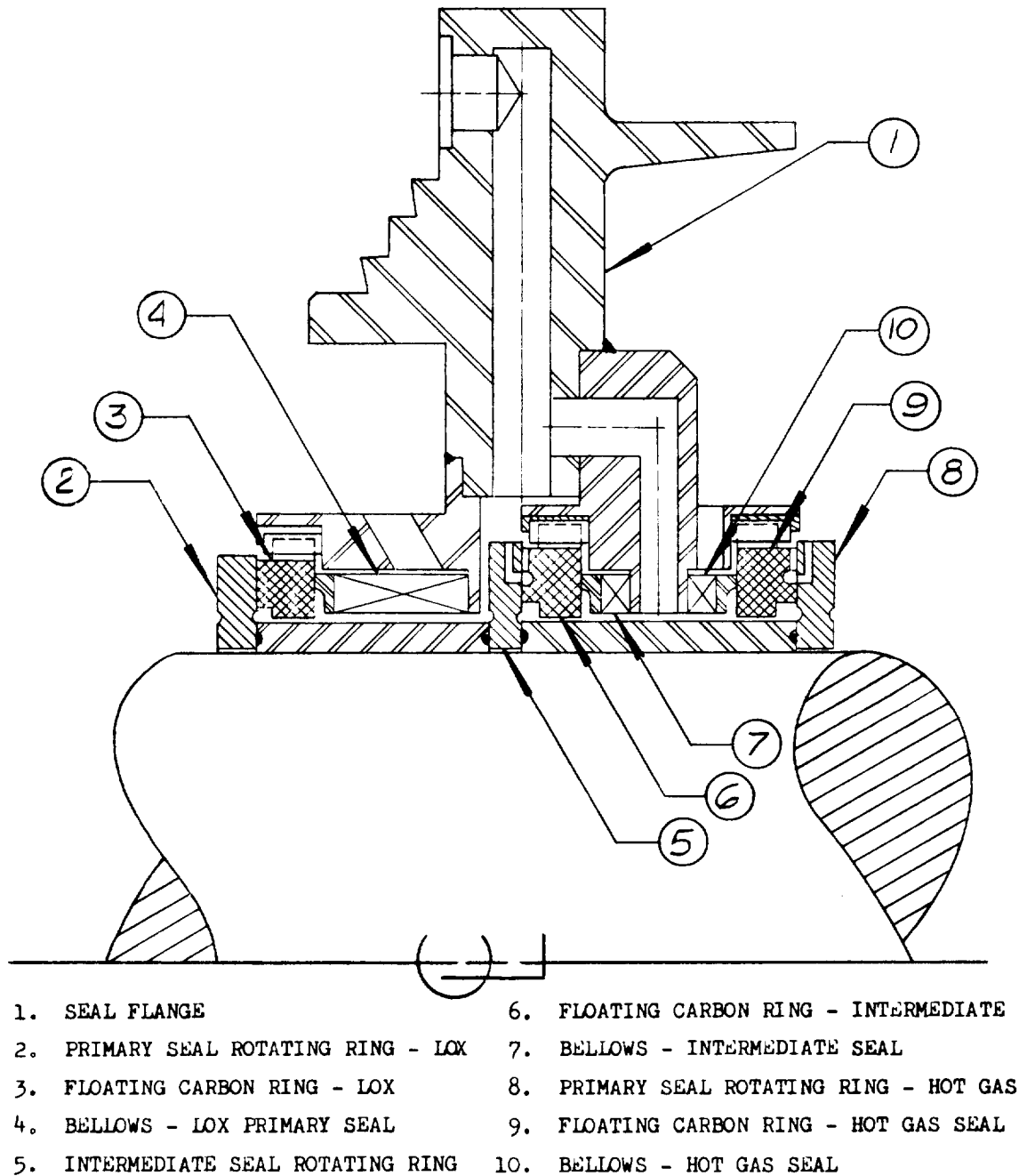


Figure 4

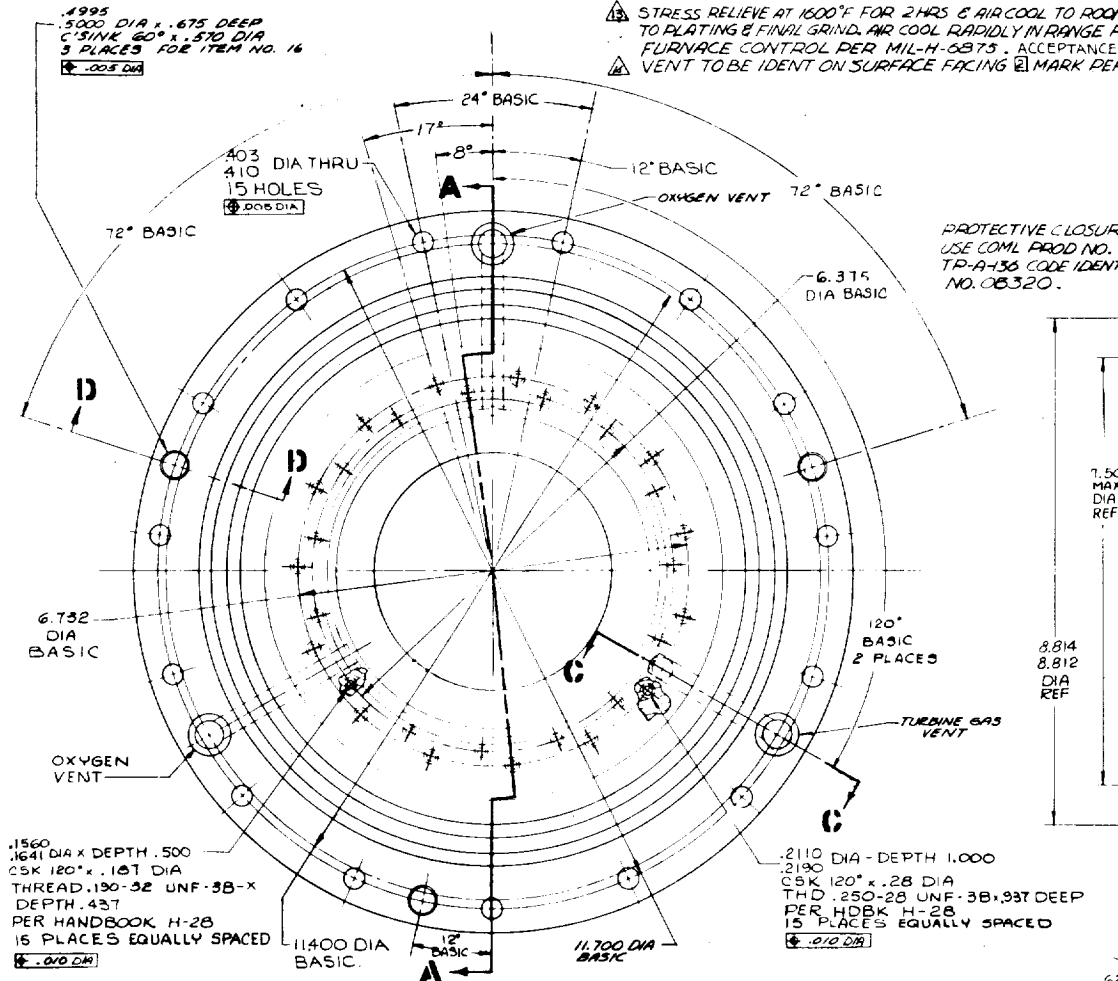


- NOTES: 1. REMOVE ALL BURRS & SHARP EDGES EQUIV TO .005/.015 R UNLESS OTHERWISE NOTED. SYMBOLS PER MIL-STD-812 AND JAN-STD-19.
2. THESE SURFACES TO BE FREE OF SCRATCHES, DENTS, PITS & FLAWS.
3. SURFACE ROUGHNESS TO BE 125 PER MIL-STD-10 UNLESS OTHERWISE NOTED.
4. MAXIMUM PERMISSIBLE RUN-OUT ON THIS SURFACE .010 T.I.R.
5. TIG WELD PER MSFC 10309308 CLASS I. RADIOGRAPHIC INSPECTION NOT REQUIRED.

7. ALL WELDS ARE TO BE FREE OF DISCONTINUITIES

8. CLASSIFICATION OF CHARACTERISTICS PER MIL-STD-1916 DENOTED BY (C) (CRITICAL), (M) (MAJOR) & (N) (MINOR).
9. CLEAN PER AGC 46350 LEVEL - H.
10. PRESERVE & PACKAGE PER MSFC 10419900 FOR LOX.
11. FLAME PLATE, PLATE SURFACE WITH LW-5 TUNGSTEN FINISH .008 THK. LINDE CO. DIV. UNION CARBIDE CORP. SAN FRANCISCO, CALIF. CODE NO. 10217.

12. PENETRANT INSPECT PER MIL-I-6866, OPTIONAL. NO CRACKS, LAPS, PITS OR : ALLOWED.
13. STRESS RELIEVE AT 1600°F FOR 2 HRS & AIR COOL TO ROOM TO PLATING & FINAL GRIND. AIR COOL RAPIDLY IN RANGE F. FURNACE CONTROL PER MIL-H-6875. ACCEPTANCE VENT TO BE IDENT ON SURFACE FACING 2 MARK PER



| OPERATING CONDITIONS  |   | STATIC CONDITIONS                        |                             |
|---|---|--|-----------------------------|
| SPEED   | 4,000 RPM. MAX  | MAXIMUM PRESSURE                         | AT 1 - 65 PSIA FOR 12 HOURS |
| ACCELERATION  | 120 REV/SEC <sup>2</sup> MAX                                  | MINIMUM PRESSURE                         | AT 2 - 0 PSIA               |
| ALLOWABLE SHAFT RUNOUT (RADIAL)   | .007 T.I.R.   | LEAK TEST (STATIC)                       |                             |
| AXIAL PLAY  | .018 TO .023  | ALLOWABLE LEAKAGE RATES (EXTERNAL PRESS) |                             |
| TEMPERATURE   |   | HELIUM GAS AT 68°F                       |                             |
| AT 1  | -250°F  | AT 1                                     | 0 CC/SEC                    |
| AT 2  | 917°F MAX.  | AT 2                                     | 0 CC/SEC                    |
| EXTERNAL PRESSURE   |   | LEGEND                                   |                             |
| AT 1  | 550 PSIA  | ⊗ = ULTIMATE DESIGN GOAL                 |                             |
| AT 2  | 80 PSIA   |  |                             |
| MEDIUM  |   |  |                             |
| AT 1  | LIQUID OXYGEN   |  |                             |
| AT 2  | HOT TURBINE GASES (90% H <sub>2</sub> + 10% H <sub>2</sub> O) |  |                             |
| NOTE: MEDIUMS AT 1 AND 2 MUST NOT BE ALLOWED TO MIX UNDER STATIC & DYNAMIC CONDITIONS |   |  |                             |
| NUMBER OF STARTS  | 30  |  |                             |
| LIFE  | 10 HOURS  |  |                             |

1. ALL BELLOWS SEAL MECHANICAL ADVISORY TEMPERATURE
2. SHAFT
3. SHAFT
4. VENDOR ON SE
- HYDRAULIC (EXTERNAL)
- MECHANICAL INSTALL COMPRE SPRING

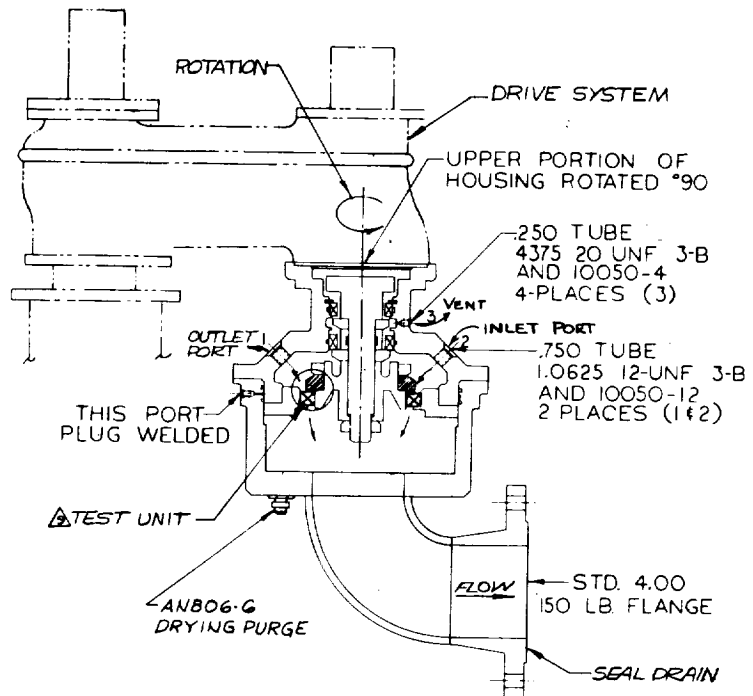






APPLICATION  
LO<sub>2</sub>  
LH<sub>2</sub>  
HOT GAS

- MOUNT



TESTER SCHEMATIC SUBASSY SEAL —  
ASSEMBLY INVERTED FOR LOW & HOT GAS

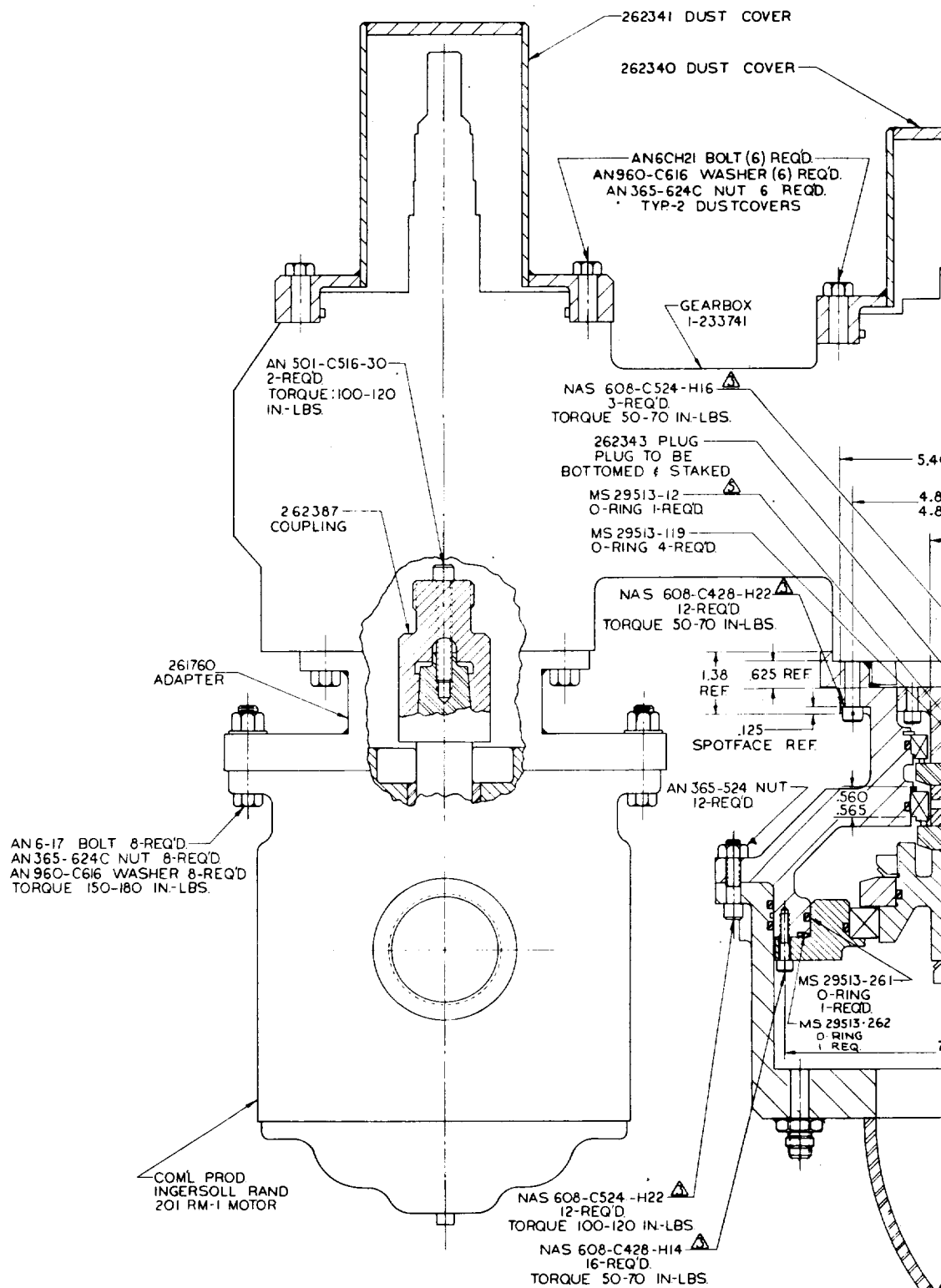
|    |  |           |           |  |  |  |  |  |  |  |
|----|--|-----------|-----------|--|--|--|--|--|--|--|
|    |  |           |           |  |  |  |  |  |  |  |
| 2  |  | M5295230  | O' RING   |  |  |  |  |  |  |  |
| 1  |  | M5295372  | D' RING   |  |  |  |  |  |  |  |
| 1  |  | 204972    | SEAL ASSY |  |  |  |  |  |  |  |
| 16 |  | M5608C4H4 | BOLT      |  |  |  |  |  |  |  |

|  |    |      |
|--|----|------|
|  | 2  |      |
|  | 1  |      |
|  | 1  |      |
|  | 1  |      |
|  | 1  |      |
|  | 1  |      |
|  | 1  |      |
|  | 1  |      |
|  | 1  |      |
|  | 12 |      |
|  | 1  |      |
|  | 1  |      |
|  | 12 |      |
|  | 1  |      |
|  | 1  |      |
|  | 2  |      |
|  | 1  |      |
|  | 2  |      |
|  | 2  |      |
|  | 12 |      |
|  | 3  |      |
|  | 1  |      |
|  | 4  |      |
|  | 2  |      |
|  | 1  |      |
|  | 1  |      |
|  | 2  |      |
|  | 1  |      |
|  | 1  |      |
|  |    | SAM. |



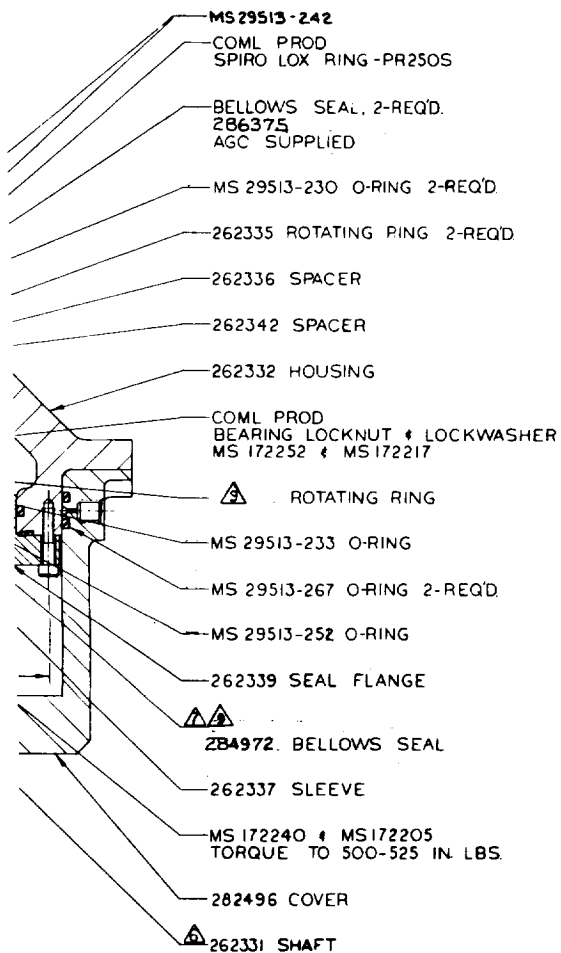








2



|       |         |        |
|-------|---------|--------|
| 05824 | E       | 261760 |
| 1     | 2-13-62 | 2 OF 2 |

Figure 6 (Sheet 2 of 2)  
Subscale Seal Test Fixture  
Page 12



head is designed to simulate the specific requirements of the full size application. Pertinent specifications are summarized as follows:

| <u>Condition</u>                      | <u>Full Size Value</u>            | <u>Sub Scale Value</u> | <u>Reason for Difference</u>          |
|---------------------------------------|-----------------------------------|------------------------|---------------------------------------|
| Rubbing Velocity                      | 115 Ft/Sec                        | 115 Ft/Sec             | ---                                   |
| Operating Pressure -<br>Liquid Oxygen | 450 psi                           | 300 psi                | Stress Limitation in<br>Bellows       |
| Operating Pressure -<br>Hot Gas       | 125 psi                           | 125 psi                | ---                                   |
| Liquid Oxygen Side Test<br>Fluid      | Liquid<br>Oxygen                  | Liquid<br>Oxygen       | ---                                   |
| Hot Gas Side Test<br>Fluid            | H <sub>2</sub> + H <sub>2</sub> O | Heated GN <sub>2</sub> | Hot Gas Availability                  |
| Bellows Preload                       | 11 psi                            | 11 psi                 | ---                                   |
| Shaft Speed                           | 4,000 rpm                         | 6,500 rpm              | To Maintain Equal Rubbing<br>Velocity |

The over-all arrangement of the test equipment and facility is shown in Figure 7.

## (2) Test Development Activity

Six combinations of nosepiece/rotating ring materials for liquid oxygen and four combinations for hot gas were evaluated. A summary of the subscale test activity is shown in Tables 1 and 2.

## (3) Test Development Results

### (a) Liquid Oxygen Application

The best results were obtained with the combination of PO3N carbon operating against a LW5 plated rotating ring. The PO3N is a pure graphite material manufactured by Pure Carbon Company and the LW5 plating consists of 25% tungsten carbide, 7% nickel, and a mixture of tungsten chromium, deposited 0.002 in. thick on Inconel X base metal by a flame plating process (Linde Company).

The next best combination was found to be P5N carbon operating against LW5 plating. The P5N carbon is a hard graphite material treated with chemical salt impregnation. It is somewhat harder than PO3N and showed evidence of heat checks on the rotating rings.

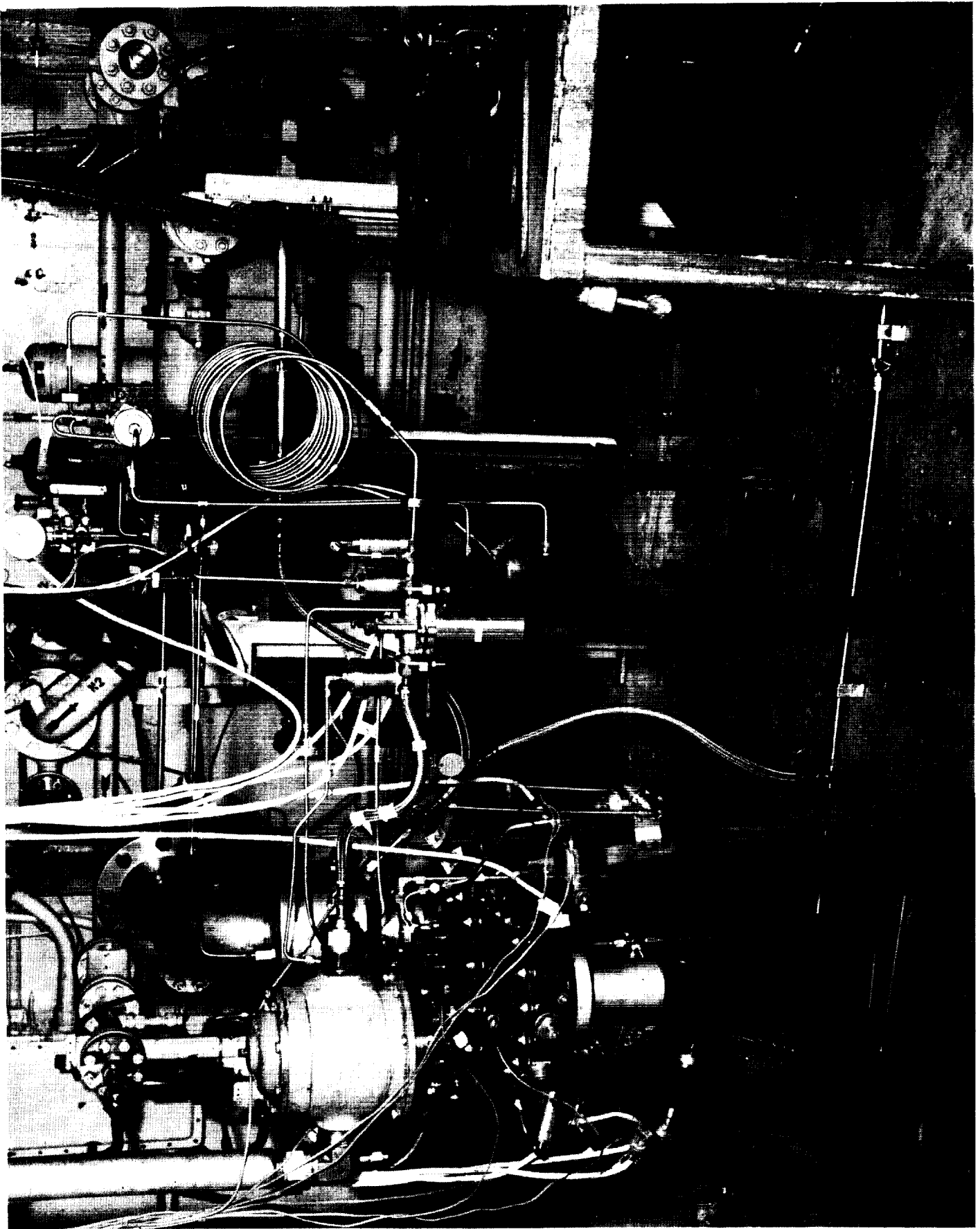


Figure 7

Subscale Seal Test Facility

TABLE 1

SUMMARY OF SEAL MATERIAL EVALUATION TESTS  
FOR LOX SEAL IN SUB SCALE SEAL TESTER

| DATE                  | MATERIAL  |               | TEST<br>DURATION<br>SEC. | TEST RESULTS                    |
|-----------------------|-----------|---------------|--------------------------|---------------------------------|
|                       | NOSEPIECE | ROTATING RING |                          |                                 |
| January/March 1963    | P03N      | LW5           | 300                      | Nosepiece and Ring Satisfactory |
| January/March 1963    | P03N      | LW-IN-30      | -                        | Nosepiece and Ring Satisfactory |
| April 1963            | P03N      | LC-LA         | 780                      | Nosepiece and Ring Satisfactory |
| April 1963            | P5N       | Chrome Plate  | 300                      | Ring Plating Failure            |
| May/June 1963         | P5N       | LW5           | -                        | Nosepiece and Ring Satisfactory |
| June/July 1963        | P03N      | LW5           | 1955                     | Nosepiece and Ring Satisfactory |
| August 1963           | P03N      | LW5           | 450                      | Nosepiece and Ring Satisfactory |
| August/September 1963 | P03N      | LW5           | 2190                     | Nosepiece and Ring Satisfactory |
| September 1963        | P03N      | LW5           | 390                      | Nosepiece and Ring Satisfactory |
| November 1963         | P03N      | Chrome Plate  | 752                      | Ring Plating Failure            |
| January 1964          | P03N      | LW5           | 727                      | Nosepiece and Ring Satisfactory |
| January 1964          | P03N      | LW5           | 1637                     | Nosepiece and Ring Satisfactory |

TABLE 2

SUMMARY OF SEAL MATERIAL EVALUATION TESTS  
FOR HOT GAS SEAL IN SUB SCALE SEAL TESTING

| DATE           | MATERIAL  |                                | TEST<br>DURATION<br>SEC. | TEST RESULTS                    |
|----------------|-----------|--------------------------------|--------------------------|---------------------------------|
|                | NOSEPIECE | ROTATING RING                  |                          |                                 |
| April/May 1963 | CDJ-83    | Chrome Plate                   | 320                      | Nosepiece and Ring Satisfactory |
| April/May 1965 | CDJ-83    | LW-5                           | 720                      | Nosepiece and Ring Satisfactory |
| May/June 1965  | EY105     | Chrome Plate,<br>Teflon Bonded | 280                      | Nosepiece and Ring Satisfactory |
| May/June 1963  | CDJ-83    | Chrome Plate                   | 257                      | Rotating Ring Failure           |
| June 1963      | EY105     | LW5, Epon<br>Bonded            | -                        | Nosepiece and Ring Satisfactory |
| September 1963 | EY105     | LW5                            | 227                      | Nosepiece and Ring Satisfactory |

The combinations of either PO3N carbon or P5N carbon running on a chrome plated rotating ring produced flaking-off of the plating and failure of the seal surfaces. Examination of the plating, after the failures, indicated excessive softness of the chromium deposit. It was concluded that the failures may have been caused by substandard chrome-plating or by excessive pressure loading of the rotating ring. Subsequent satisfactory performance of P5N carbons with the full scale chrome plated rotating rings supports this conclusion because no failures occurred with full scale rings plated by the Sealol Company.

In general, heavier transfer of carbon from the nosepiece to the rotating ring was experienced with chrome plated rings than with LW-5 plated rings.

#### (b) Hot Gas Application

Both CDJ-83 and EY105 in combination with LW-5 plating appeared to be satisfactory. CDJ-83 is a carbon material manufactured by the National Carbon Company, and EY105 is a carbon material made by Morganite, Inc. The chrome plating failed with CDJ-83, but this failure was probably also the result of the improper application of plating.

#### (c) Carbon to Retainer Bonding

Unlike the liquid oxygen seal, where the differential expansion between the carbon and its retainer causes a tighter fit and a better retention of the carbon, thermal effects in the hot gas seals produce the opposite effect of loosening the carbon fit. This necessitates bonding of carbon to its retainer. Two materials, Teflon and Epon 422, were evaluated for this application. Teflon failed after 400 sec operation and this failure was evidenced by the extrusion of Teflon from the bond indicating that the nosepiece had not been fully sealed in the retainer. Performance of the Epon 422 appeared to be satisfactory.

### b. Full Scale Seal Testing

#### (1) Test Equipment

The general arrangement of the test equipment is shown in Figure 8 and Figure 9. Initially, the test ring was similar to the previously described sub scale tester, but as a result of test experience, the drive was modified from an air motor to a more powerful gaseous nitrogen turbine drive with automatic speed control for close simulation of turbopump operating conditions. The tester was operated in the Aerojet-General Corporation Cryogenics Laboratory where a liquid oxygen supply at required pressures up to 450 psi was available from a 1,000 gallon storage tank. Seal leakage was vented via manifold lines and passed through a flow measuring system to exhaust outside of the test cell. Originally, a volumetric displacement system was intended for measuring leakage. This was found inadequate for the application and a flowmeter system was designed and purchased; however, it was installed only a short time before the termination

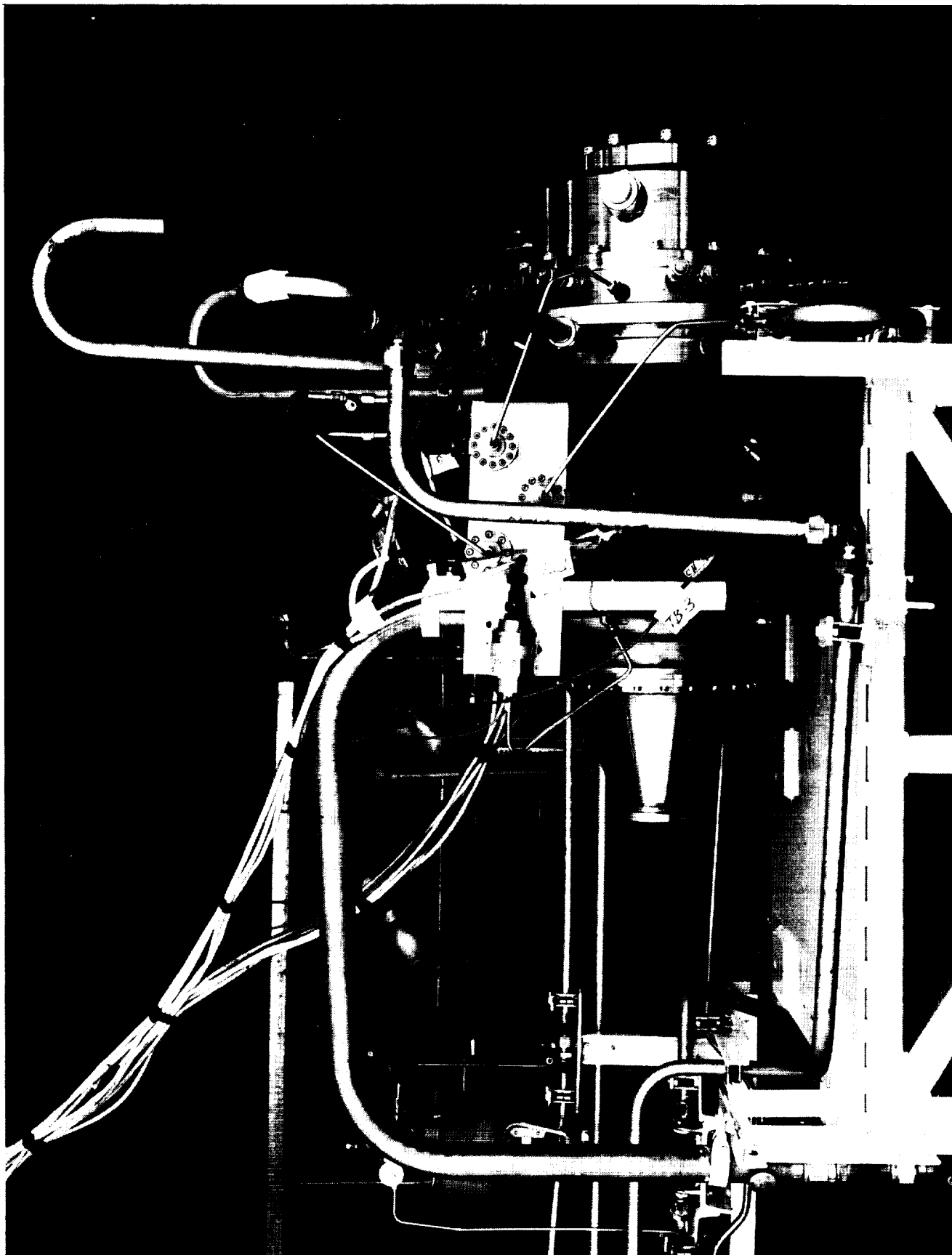


Figure 8

Full Scale Seal Test Facility

2. INTERPRET DWS REP STANDARDS  
AS PRESCRIBED IN MIL-D-10332Z
3. LOCKWIRE REP AGC-4637, CLASS 1A
3. MATCH MARK ALL PARTS BEFORE  
DISASSEMBLY.
4. CLEAN REP AGC-4635, LEVEL E.
5. MARK REP ASD-5715 W/ WITH PART NO.  
23472 & APPLICABLE DASH NO.

- 
- Exploded view diagram of the rear of a 1983 Chevrolet 1500. The diagram shows the rear axle assembly, including the axle housing, axle, brake drum, and various mounting brackets and bolts. Callouts 71, 72, 73, 74, and 75 point to specific components. Callout 75 includes the text "TORQUE TO 180 IN LB".

DETAIL 13  
-39 ASSY

76 TORQUE TO 180 IN. LB

57 TORQUE TO 180 IN. LB

73 71 77 75 74

DETAIL 13 24  
-49 ASSY

Diagram illustrating the rear suspension assembly components and their torque specifications:

- 56**: TORQUE TO 100-120 IN.LBS
- 57**: TORQUE TO 180 IN.LBS
- 52**: Upper control arm
- 53**: Lower control arm
- 54**: Shock absorber
- 55**: Spring plate
- 58**: Rear axle
- 59**: Rear wheel hub

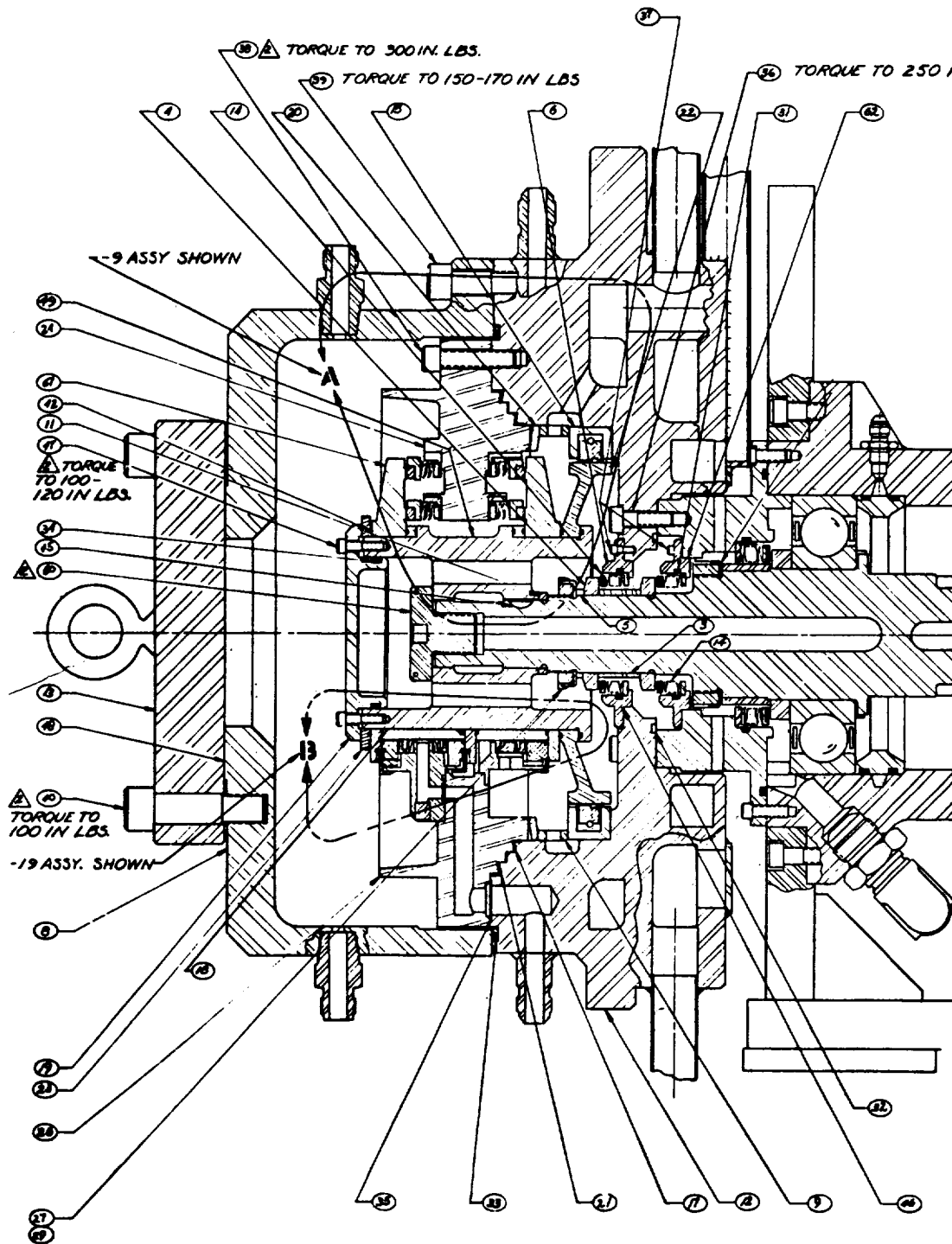
DETAIL 13 58  
-29 ASSY

[illegible]



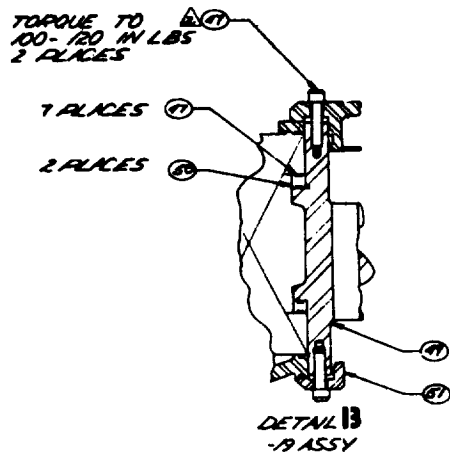








2



LBS.

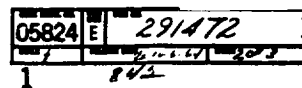
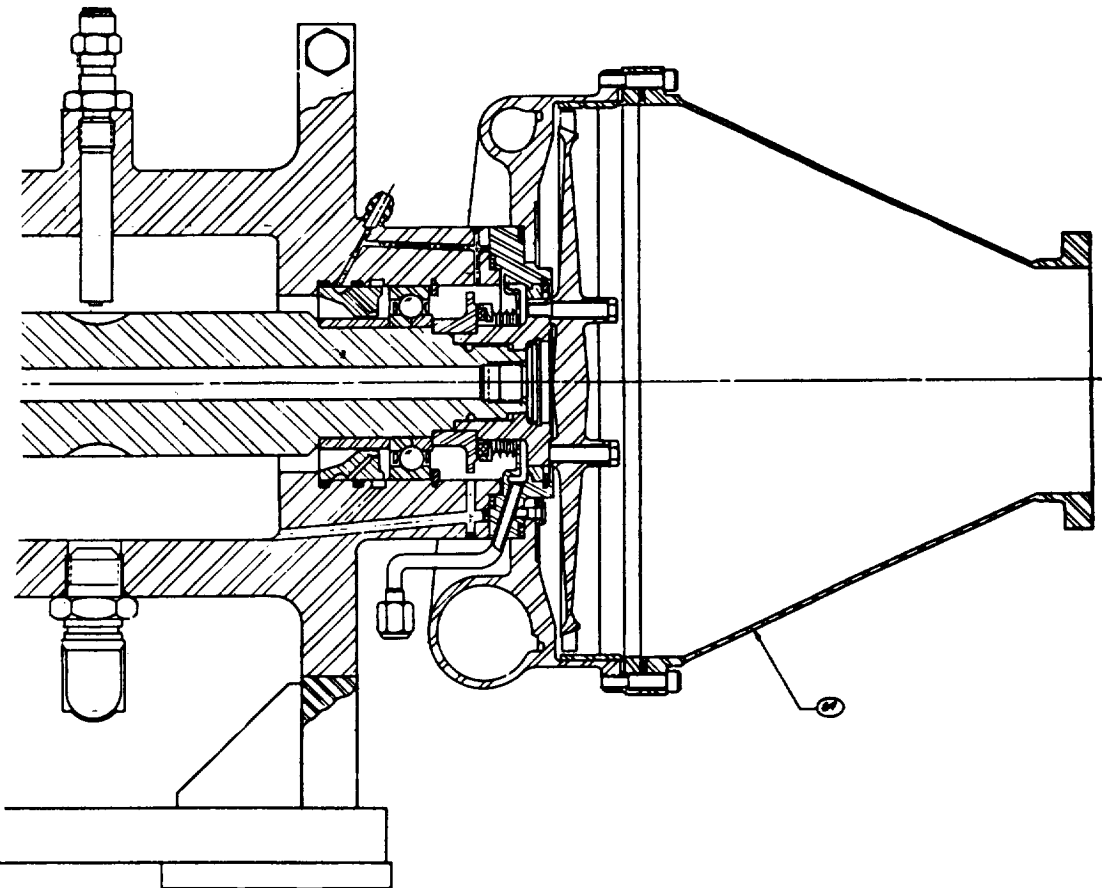


Figure 9 (Sheet 2 of 3)

Full-Scale Seal Tester







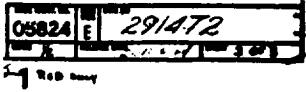
2

| TESTER SPECIFICATIONS |        |        |        |        |
|-----------------------|--------|--------|--------|--------|
| APPLICATION           | TESTER | TESTER | TESTER | TESTER |
| HOT GAS               | 150    | 0      | 1600   | 120    |
| LD                    | 150    | 0      | 1600   | 120    |

NOTE: LD TESTS & HOT GAS TESTS  
TO BE SEPARATE



STD 4.0 IN.





of the testing and had not contributed to the leakage rate evaluation. All leakage rates throughout the program were calculated from the flow continuity equation based upon cross-sectional area, pressure, and temperature of the leaking gas.

## (2) Test Development Activity

Six test series were completed between February and September 1964. Four seal assemblies were used in the program and 8,650 seconds of operational time was accumulated. The test activity was carried out in two phases.

### (a) Phase I - Preliminary Evaluation of the Sealol Seal Performance

Two seals (D/N 280115, S/N 20 and S/N 22) were used and the seal testing was combined with test equipment shakedown and instrumentation evaluation activity. This activity covered the period from February to April 1964. A typical prototype seal is shown on Figure 10.

### (b) Phase II - Investigation of the Causes of High Leakage Rates through the Primary Liquid Oxygen Seal

Three seals were used, the Sealol seal (P/N 280115, S/N 19 and S/N 23), and the Borg Warner seal (P/N 284938, S/N 002). This activity covered the period from April through June 1964.

A chronological summary of the above Phase I and Phase II test activity is given in Table 3.

## (3) Test Development Results

### (a) Phase I - Preliminary Evaluation of the Sealol Seal

The results from the first tests of Sealol seals (S/N 20 and S/N 22) at 4,000 rpm and 400 psi in liquid oxygen indicated an average seal face carbon wear rate of 0.005 in. per 1,000 sec. This average was based upon a total operating time of approximately 4,000 sec and was considered satisfactory at the time. The leakage rate across the primary liquid oxygen seal was in the order of  $1.6 \times 10^6$  scc/min, rather than the maximum of 30,000 scc/min allowed by specification. As a result of this high leakage, a back pressure of approximately 100 psi developed in the primary seal vent line causing further unacceptably high leakage across the secondary liquid oxygen seal. Subsequent testing was directed toward establishing the causes of the unacceptable high leakage rates. The following possible causes were considered:

1 Vibration of the seal, causing separation of the carbon seal nosepiece and the rotating ring.

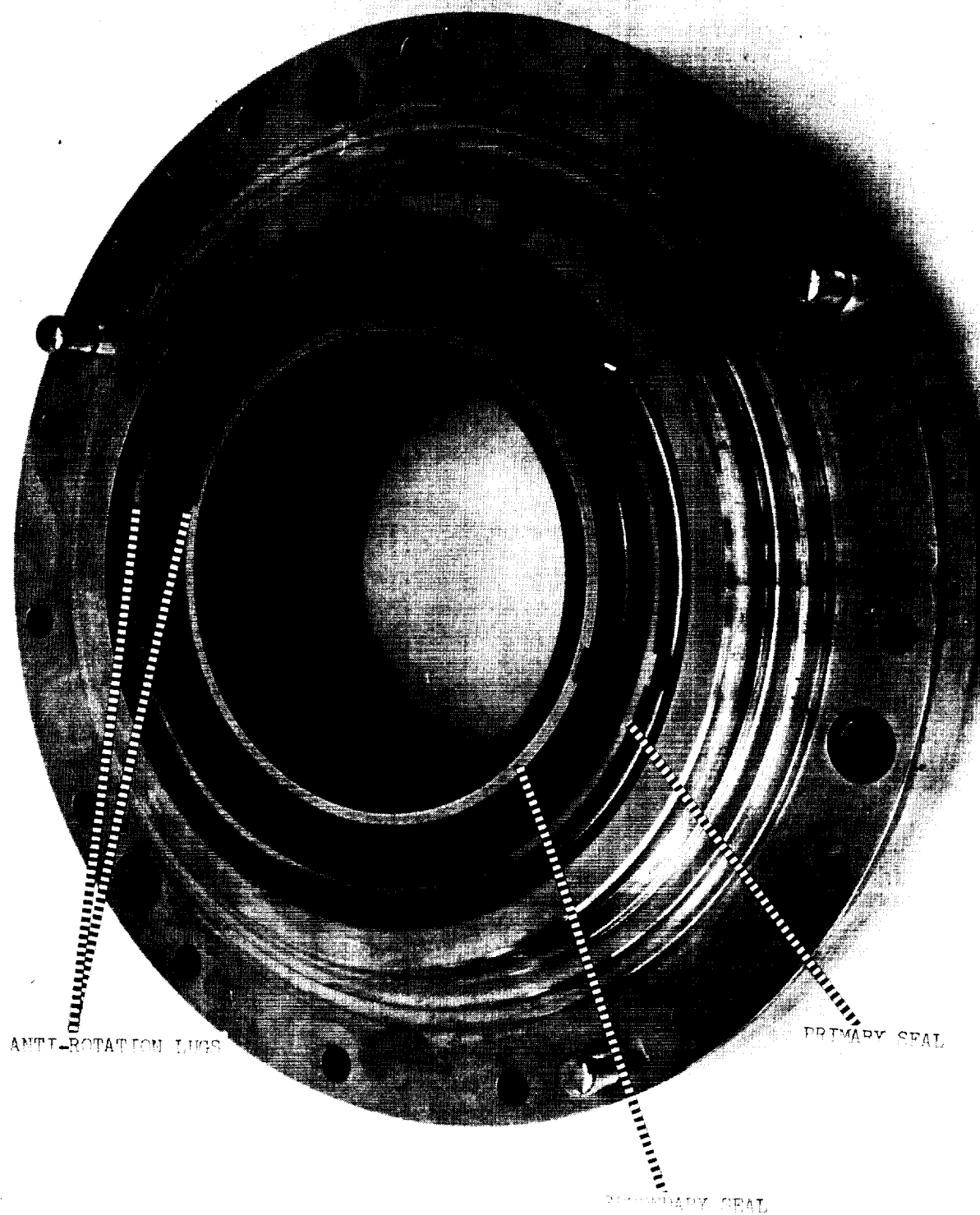


Figure 10

Typical Prototype Seal

TABLE 3

## SUMMARY OF PROTOTYPE SEAL TESTS

| <u>DATE</u>      | <u>SEAL AND S/N</u> | <u>TEST DURATION - SEC</u> | <u>TEST OBJECTIVES</u>  |
|------------------|---------------------|----------------------------|---|
| 13 February 1964 | Sealol S/N 22       | 4060                       | Seal Evaluation   |
| 1 April 1964     | Sealol S/N 19       | 280                        | Evaluation of Non-Interference<br>Fitted Nosepiece                      |
| 20 April 1964    | S/N 20, Sealol      | 1260                       | Seal Evaluation   |
| 7 May 1964       | Sealol S/N 23       | Static Leakage Checks      | Evaluation of Effect of<br>Thermal Cycling                              |
| 25 May 1964      | Sealol S/N 23       | 659                        | Test in LN <sub>2</sub> Evaluation of<br>Effects of                     |
| 1 June 1964      | Sealol S/N 23       | -                          | Test in H <sub>2</sub> O Boiling and                                    |
| 2 June 1964      | Sealol S/N 23       | -                          | Test in GN <sub>2</sub> Non-Boiling<br>Fluids                           |
| 8 June 1964      | Sealol S/N 20       | Static                     | Evaluation of Large Vents (Static)                                      |
| 9 June 1964      | Sealol S/N 20       | 647                        | Evaluation of Large Vent (Dynamic)                                      |
|                  | Borg Warner         | 1740                       | Evaluation of Borg-Warner Concept<br>and Evaluation of 76% Over-Balance |

2 Distortion of the carbon nosepiece caused by thermal or mechanical stresses and dimensional instability of the carbon retainer assembly.

3 Excessive back pressure in the primary seal vent line.

4 Unstable pressure conditions on the sealing surface caused by boiling of liquid oxygen across the seal contact face.

5 Incorrect seal face loading.

(b) Phase II - Investigation of Possible Leakage Causes

1 Vibration

The natural frequency of the undamped seal and the vibratory characteristics of a damped seal were determined by the frequency survey method on a shake table. When the seal bellows was compressed axially, as in the turbopump or tester installation, the lowest vibrational mode was the axial oscillation of the middle part of the bellows, with no movement of the carbon nosepiece. The vibration frequency was approximately 333 cycles per second, which is five times higher than the maximum shaft operating frequency of 66 cycles per second. The addition of 11 U-shaped dampers uniformly spaced around the seal circumference causes a frequency reduction to 269 cycles per second. The damped configuration was tested dynamically at design speed and pressure with no noticeable reduction in the previously experienced leakage of  $1.6 \times 10^6$  scc/min. From this, it was concluded that the addition of dampers had no effect upon leakage, although they will most likely be beneficial in preventing bellows fatigue failures.

2 Distortion of Carbon Nosepiece and Rotating Ring

This was investigated in two ways;

a By making a direct measurement of flatness before and after test.

b By eliminating the influence of thermal and mechanical stresses upon leakage rates in actual tests.

Electronic type surface gages capable of measuring surface deviations of the order to 10 micro-inches were used to determine the flatness of the carbon nosepiece and of the rotating ring prior to installation and after disassembly. The typical surface flatness of a lapped carbon is shown in Figures 11 and 12. These indicate that the seal is typically saddle-shaped with two broad concavities 200 to 400 micro-inches deep, spaced approximately 180 degrees apart. The stiffness of the nosepiece is extremely low and light



SURFACE FLATNESS OF PRIMARY LOX SEAL CARBON  
TALY ROND MEASUREMENT, SEAL S/N 020, SEP 8, 1964.

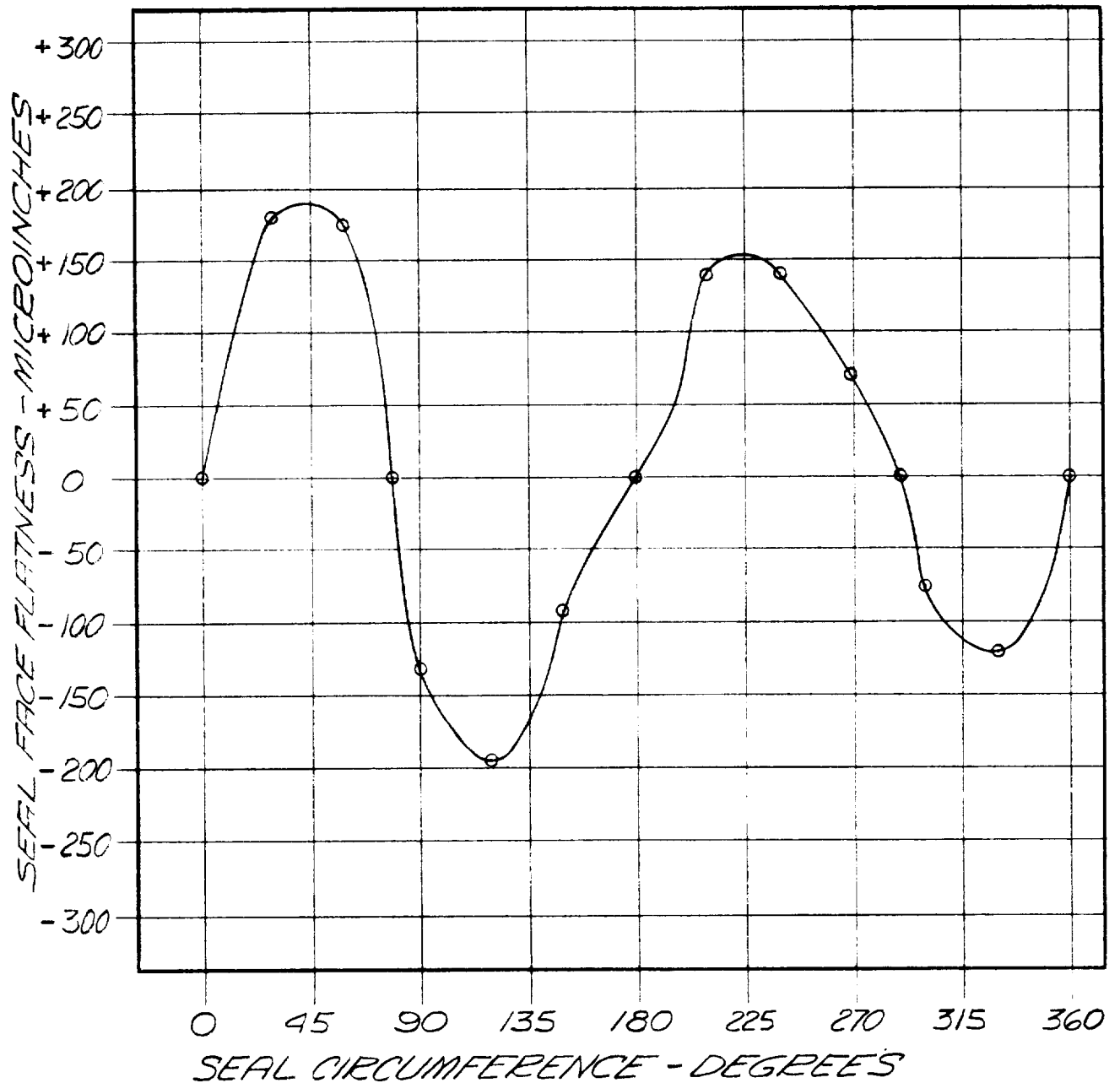


Figure 12

Lapped Seal Face Talyrond Surface Measurement

local pressures (finger pressure) can easily change surface topography. The loading by the stylus of the measuring instrument is 0.10 gram which is considered negligible.

In contrast, the flatness of the rotating ring is typically within 25 micro-inches and remains constant under normal handling conditions. However, during operation, transfer of carbon to the rotating ring occurs, causing the surface to be no better than 100 micro-inches in flatness.

It appears, then, that the flexibility of the 7 in. diameter, 1/4 in. thick carbon nosepiece is such that it can easily change its shape under local forces. If these forces are uniformly distributed circumferentially, the effect would be to flatten the carbon against the rotating ring. However, if a local interfacial force arises between the carbon and the ring, caused, for example, by liquid boiling or a hydrodynamic film, it can easily distort the sealing surface locally.

The effect of thermal and pressure stresses was investigated in a gross manner by replacing the carbon nosepiece, which is normally installed with 0.010-in. radial interference and operates with 0.017-in. interference at cryogenic temperatures, with a Teflon bonded insert installed with 0.005-in. radial clearance. When tested at design speed and pressure, this seal did not show any improvement in the leakage.

A seal with an interference fitted carbon was subjected to 13 chill and heat cycles (from -320°F liquid nitrogen temperature to +100°F gaseous nitrogen temperature) while stationary. While the leakage increased somewhat with the number of cycles, it did not exceed the value normally found in randomly selected unused seals.

### 3 Excessive Back-Pressure in the Primary Seal Vent

Larger than expected leakage rates from primary seal caused buildup of the back-pressure (up to 100 psig) in the 3/8-in. diameter vent line. To reduce this pressure to the desired value of 1 psig or less, the vent size was enlarged from 0.11-in.<sup>2</sup> to 1.8-in.<sup>2</sup> When this configuration was tested, it was found that the leakage rate from the primary seal dropped from  $1.6 \times 10^6$  scc/min to approximately  $0.8 \times 10^6$  scc/min with pressure in the vent line never exceeding 3 psig.

This result appears to be in conflict with the basic flow equation,  $Q = CA \left( 2g \frac{\Delta P}{\rho} \right)^{1/2}$ , which states that the lowering of the back pressure should have produced a greater leakage instead of an improvement. However, it may be reasoned that a higher back pressure will alter the assumed pressure profile across the sealing surface and the hydraulic balance, thereby providing the conditions for an enlargement of the leakage gap between the seal faces. In addition to this, the heat generation resulting from seal face rubbing, possibly causing a phase change in the liquid, can likely produce effects that influence and greatly change the pure and fundamental relationship of flow,  $Q = f(\Delta P)$ .

#### 4 Liquid Oxygen Boiling on the Seal Face

The effects of liquid oxygen boiling between the seal surfaces was investigated by comparisons with gaseous nitrogen and water under static and dynamic conditions. It was found that the leakage increased by a factor of 10 to 20 when gaseous nitrogen at 450 psi is replaced by either liquid nitrogen or liquid oxygen, and that this factor increased to 400 when the shaft was rotated at 4,000 rpm. In contrast to this, the gaseous nitrogen static leakage increased only by a factor of 2 when the shaft is rotated at 4,000 rpm. No leakage at all was recorded in the tests at static and dynamic conditions with water as a medium.

The differences in static leakage can be roughly correlated to the differences in density and viscosity of the respective fluids.

It was concluded that approximately a ten-fold increase in the leakage of the cryogenic liquid, when the shaft is rotating at 4,000 rpm, must have been caused by the rotational effects. Either generation of hydrodynamic films or generation of pressure separation forces and vibration resulting from liquid boiling between the surfaces must be postulated.

#### 5 Loading of the Seal Face

The degree to which the overbalance affects the leakage was investigated somewhat indirectly by comparing the leakage obtained in the test of the Sealol seal having 92% overbalance to that of the Borg-Warner seal with 76% overbalance. The comparison is as follows:

| <u>Seal Vendor</u> | <u>% Overbalance</u> | <u>Leakage at 4,000 rpm and 450 psi</u> |
|--------------------|----------------------|---|
| Sealol             | 92                   | 800,000 scc/min                         |
| Borg-Warner        | 76                   | 500,000 scc/min                         |

By using 50% overbalance as a basis for a fully balanced seal, the above data might be correlated as follows:  $\frac{92-50}{76-50} \frac{800,000}{500,000}$ ; this is probably just coincidence.

It was concluded that while comparison may not be entirely appropriate because of other design differences, the degree of difference in excessive seal leakage is small when compared to the 30,000 scc/min maximum leakage allowed by specification.

#### c. Effective Diameter Test Measurements

##### (1) Terminology

The term "effective diameter," a commonly used parameter of a dynamic seal bellows, defines the equivalent of the piston diameter considering

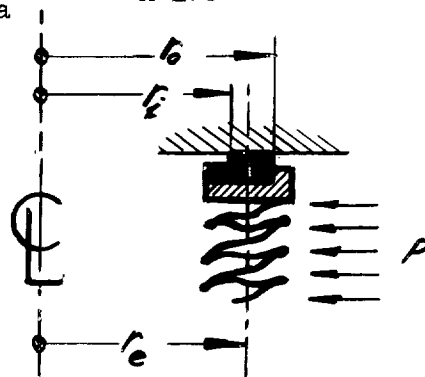
the seal bellows as a fluid actuated cylinder. The relationship between "effective diameter" and seal face loading is expressed in percentage of seal face overbalance:

$$\text{Seal Face Balance} = \frac{\text{Exposed Hydraulic Annulus Area}}{\text{Total Seal Face Area}} \times 100$$

$$= \frac{A_A}{A_F} \times 100$$

Where:  $A_A = \pi (r_o^2 - r_e^2)$

And:  $A_F = \pi (r_o^2 - r_i^2)$



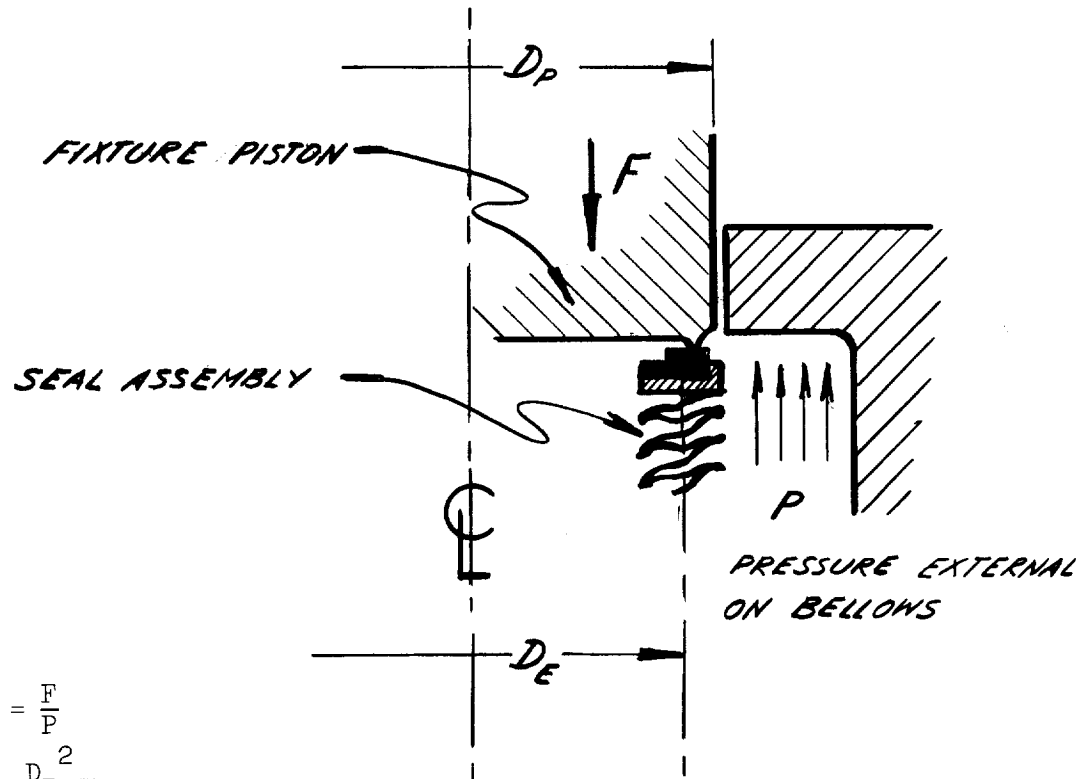
From this relationship it can be seen that if the location of the "effective diameter" divides equally the total seal face area ( $A_A = 0.5 A_F$ ), the seal face balance is  $\frac{0.5}{1} \times 100 = 50\%$ . For another example, if the "effective diameter" coincides with the inside diameter of the seal face of an externally pressurized seal,  $\frac{A_A}{A_F} \times 100 = \frac{1}{1} \times 100 = 100\%$ . This is also called "overbalance" in common usage industry terminology.

From this, it can be seen that the bellows "effective diameter" is an important parameter because of its direct influence upon seal face balance. Because seal face balance directly affects face loading, which, in turn, affects seal face wear and leakage, accurate measurement of this parameter is important in controlling the performance characteristics of bellows type dynamic seals.

## (2) Measurement System

In devising a system suitable for measuring the "effective diameter" of a seal, it must be recognized that the "effective diameter" is a parameter of the seal bellows and represents a boundary of a hydraulic pressure area normal to the axis of the bellows. While it is not possible to measure this dimension directly, it can be solved by designing an arrangement for pressurizing an annulus area between the boundaries of this unknown "effective diameter" and a fixture piston diameter of known size. If the force that is acting upon this annulus area, as a result of fluid pressurization, is measured, the area of this annulus can be calculated. By knowing the annulus area and one boundary diameter of this annular area, the other boundary diameter, the "effective diameter," can be computed.

The foregoing, expressed mathematically, is as follows:



$$\text{Annulus Area, } A_A = \frac{F}{P}$$

$$\text{Piston Area, } A_P = \frac{D_P^2 \pi}{4}$$

$$\text{Effective Diameter, } D_E = \left( D_P^2 - \frac{4F}{\pi P} \right)^{\frac{1}{2}}$$

A typical mechanical design arrangement based upon this principle is shown in Figure 13. One notable feature is the elimination of mechanical friction of the fixture piston.

### (3) Equipment

A seal test fixture, based upon the measuring system described above, was designed for determining the "effective diameter" of each of the four bellows of the Sealol seal. Figure 14 shows the test fixture set up for the primary seal bellows, and Figure 15 for the secondary seal bellows. (The piston O-rings shown on these drawings, PC No. 12 and 21 respectively, were not used during testing; therefore packing friction was eliminated.) The seal test fixture is operated in an Instron Universal Testing Machine. This machine incorporates an electronic load weighing system, a precision cross-head travel control, and strip chart data recording instrumentation. The facility also includes a 500 psig gaseous nitrogen pressure supply for seal pressurization in the fixture and "Heise" pressure gages for precision fluid pressure measurements. The equipment

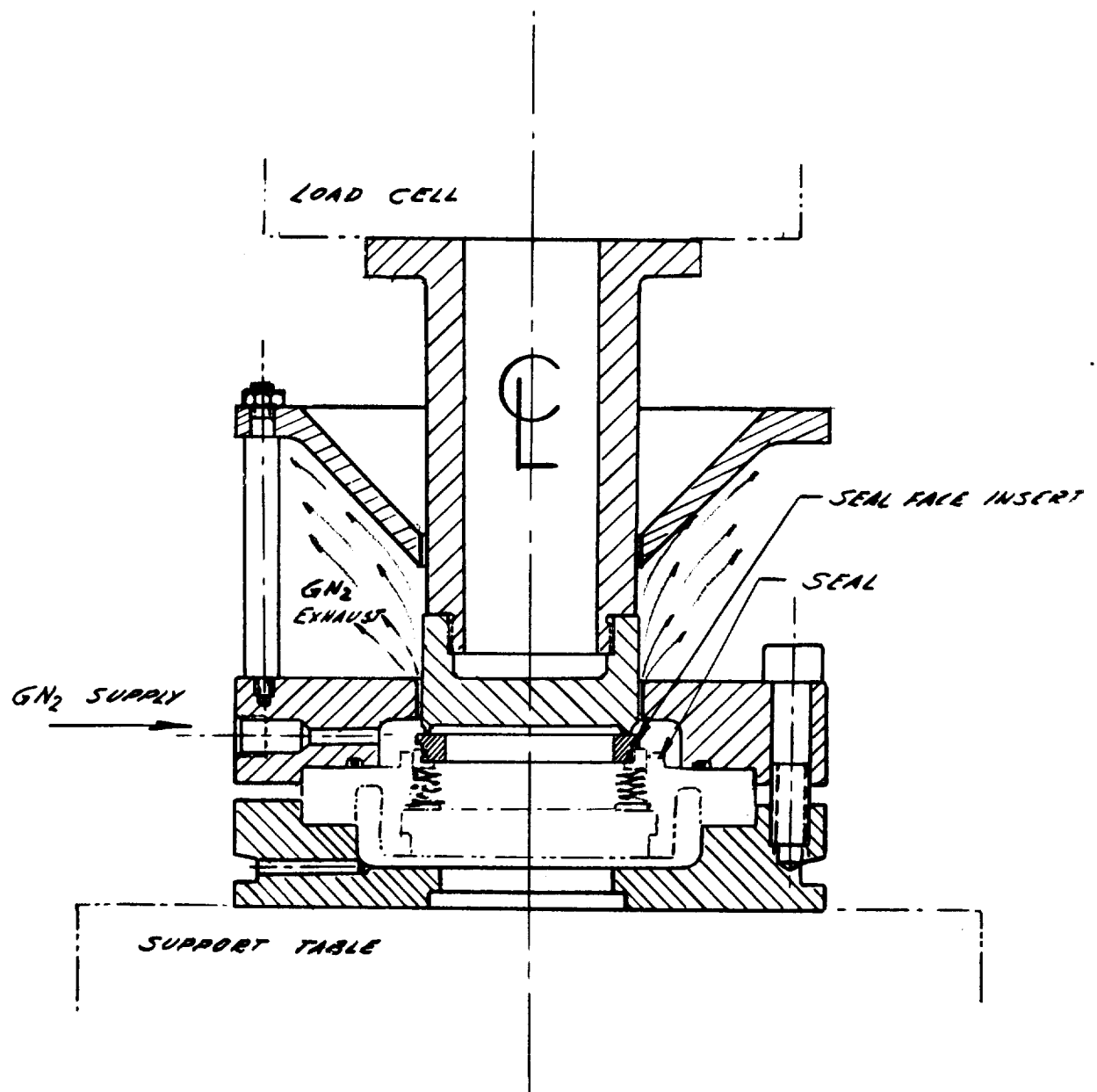


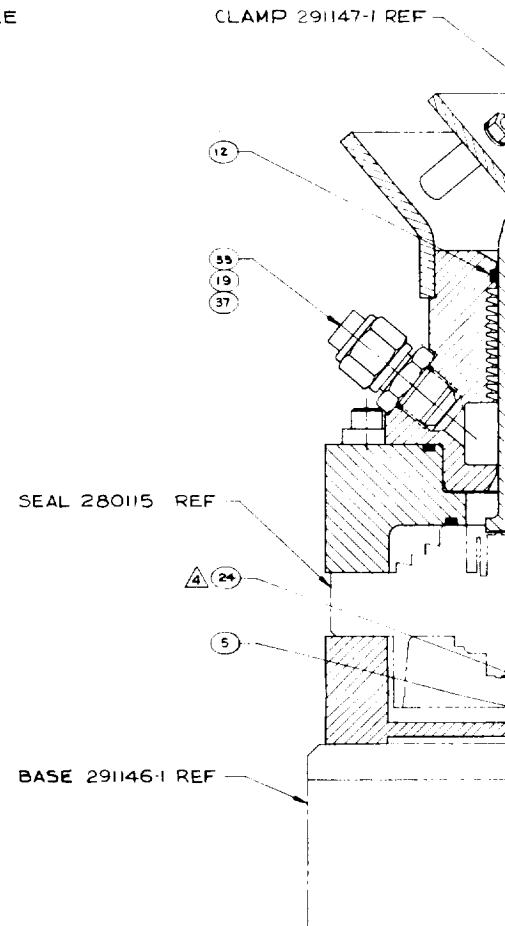
Figure 13

Typical Effective Diameter Seal Test Fixture



NOTES:

1. INTERPRET DWG PER STANDARDS PRESCRIBED IN MIL-D-70327.
2. CLEAN PER AGC 46350, LEVEL H.
3. PRESERVE AND PACKAGE PER MSFC DWG NO. 10419900 FUSELAGE COMPONENTS.
- △ BOLT TORQUE & BOLTING SEQUENCE PER TEST INSTRUCTIONS OF DEPT 9690 COGNIZANT ENGINEER.
5. THIS FIXTURE TO BE USED ONLY FOR THE PURPOSE DEFINED BY DEPT 9690 TEST INSTRUCTIONS.
6. WITH ITEM NO. 43 REMOVED AND ALL PORTS BLOCKED HYDROSTATIC TEST PER SOP 8000 AT 1000 PSIG  $\pm 10$  PSIG ITEMS NO. 6, 8, 22 & 27 (ASSEMBLED) AND ITEMS NO. 7, 8, 22 & 27 (ASSEMBLED). O-RING LEAKAGE ACCEPTABLE.
- △ AFTER HYDROSTATIC TESTING MARK ITEM NO. 6, 7 & 8 WITH "500 PSIG MAX OPERATING PRESSURE" PER ASD5215C.
8. THIS KIT TO BE USED WITH SEAL NO. 280115.
9. HYDROSTATIC TEST FIXTURE TO BE DESIGNED IN A MANNER THAT WILL ALLOW ITEM NO. 27 TO SEE FULL PRESSURE & TO HAVE APPROVAL OF COGNIZANT ENGINEER DEPT 9690 PRIOR TO TESTING.
- △ RUPTURE DISC FOR THIS ASSY TO BE ALUMINUM FOR A RUPTURE PRESSURE OF 650 PSIG AT 72° F.





CROSSHEAD - INSTRON TESTING MACHINE REF  
 INSTRON T6-47 ADAPTER REF  
 LOAD CELL - INSTRON TESTING MACHINE INSTRON P/N D31-4 REF  
 COMPRESSION TABLE 291277-1 REF

4  
 2b 4  
 40 2 REQD  
 41  
 10  
 11  
 9  
 25 4  
 40  
 8  
 22  
 6  
 20  
 2  
 3

|    |    |   |
|----|----|---|
| 10 | 1  | 1 |
| 12 | 12 |   |
| 3  | 3  |   |
| 3  | 3  |   |
| 3  | 3  |   |
| 3  | 3  |   |
| 3  | 3  |   |
| 15 | 15 |   |
| 12 | 12 |   |
| 3  | 3  |   |
| 1  | 1  |   |
| 1  | 1  |   |
| 3  | 3  |   |
| 3  | 3  |   |
| 3  | 3  |   |
| 1  | 1  |   |
| 1  | 1  |   |
| 3  | 3  |   |

SECTION A-A 

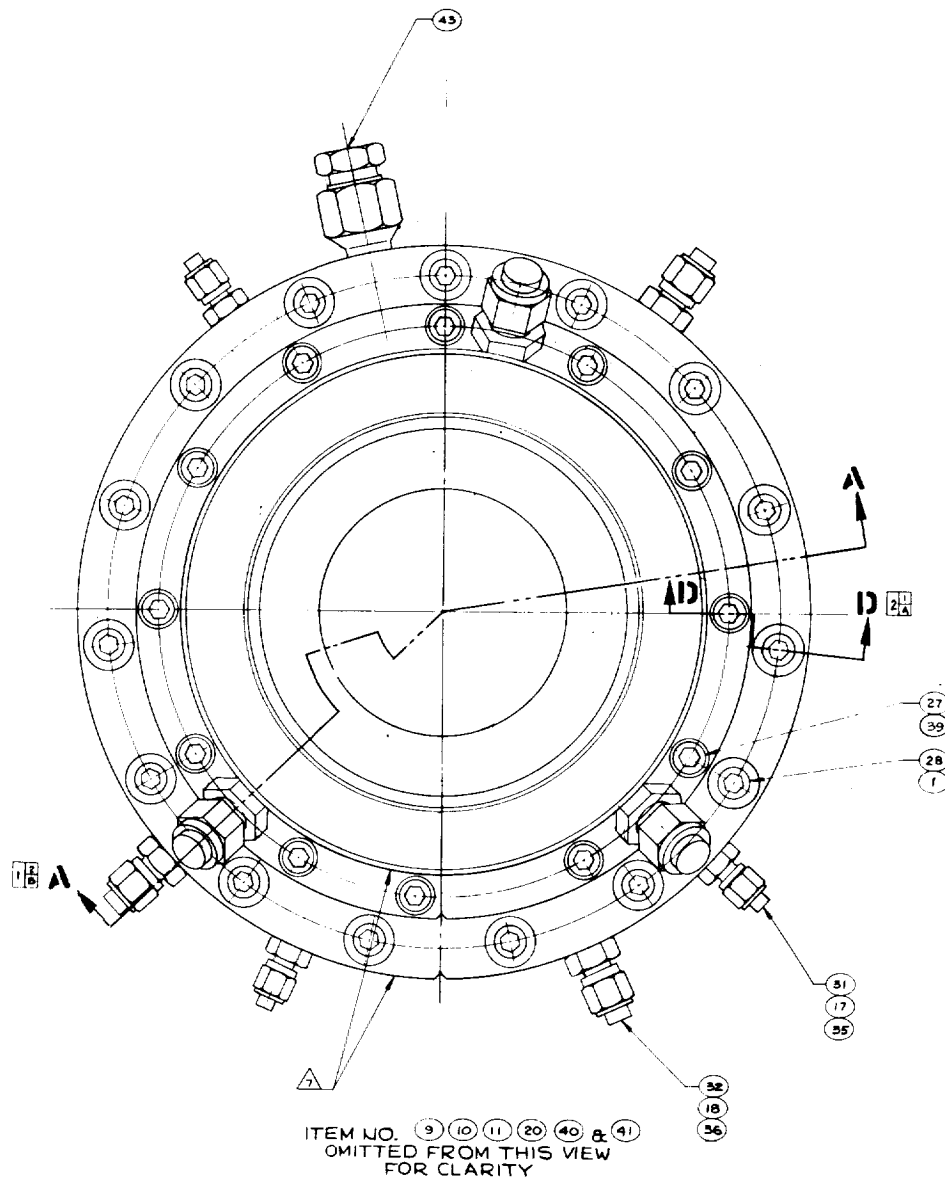
|   |   |
|---|---|
| 2 | 2 |
|   | C |

[illegible]

NO CHECK | W.O. 0617-35-810 2690 RM

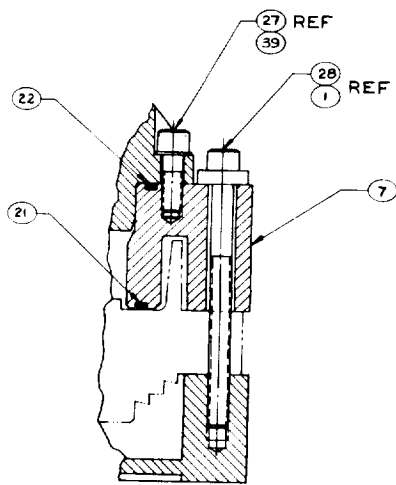
Figure 14 (Sheet 1 of 2)  
Effective Diameter Tester  
Page 33







2



SECTION D-D 22  
-19 ASSY

|       |          |        |
|-------|----------|--------|
| 05824 | E        | 291482 |
| 1/1   | 28-38-44 | 8 OF 2 |

Figure 14 (Sheet 2 of 2)  
Effective Diameter Tester  
Page 34



NOTES:

- 1 INTERPRET DWG PER STD PRESCRIBED IN MIL-D-70327.
- 2 BOLT TORQUE & BOLTING SEQUENCE PER TEST INSTRUCTIONS OF DEPT 9690 COGNIZANT ENGINEER.
- 3 THIS FIXTURE TO BE USED ONLY FOR THE PURPOSE DEFINED BY DEPT 9690 TEST INSTRUCTIONS.
- 4 WITH ITEM NO. 40 REMOVED & ALL PORTS BLOCKED HYDROSTATIC TEST PER SOP 8000 AT 1000 PSIG  $\pm 10$  PSIG ITEM NO. 4, 7, 20 & 25 (ASSEMBLED) & ITEM NO. 5, 7, 20 & 25 (ASSEMBLED) O-RING LEAKAGE ACCEPTABLE.
- 5 AFTER HYDROSTATIC TESTING MARK ITEM NO. 4, 5 & 7 WITH 500 PSIG MAX OPERATING PRESSURE PER ASD5215C.
- 6 THIS KIT TO BE USED WITH SEAL NO. 280115.
- 7 HYDROSTATIC TEST FIXTURE TO BE DESIGNED IN A MANNER THAT WILL ALLOW ITEM NO. 25 TO SEE FULL PRESSURE & TO HAVE APPROVAL OF COGNIZANT ENGINEER DEPT 9690 PRIOR TO TESTING.
- 8 RUPTURE DISC FOR THIS ASSY TO BE ALUMINUM FOR A RUPTURE PRESSURE OF 650 PSIG AT 72°F.
- 9 CLEAN PER AGC 46350, LEVEL 'H'.
- 10 PRESERVE & PACKAGE PER MSFC DWG NO. 10413900 FUSELAGE COMPONENTS.

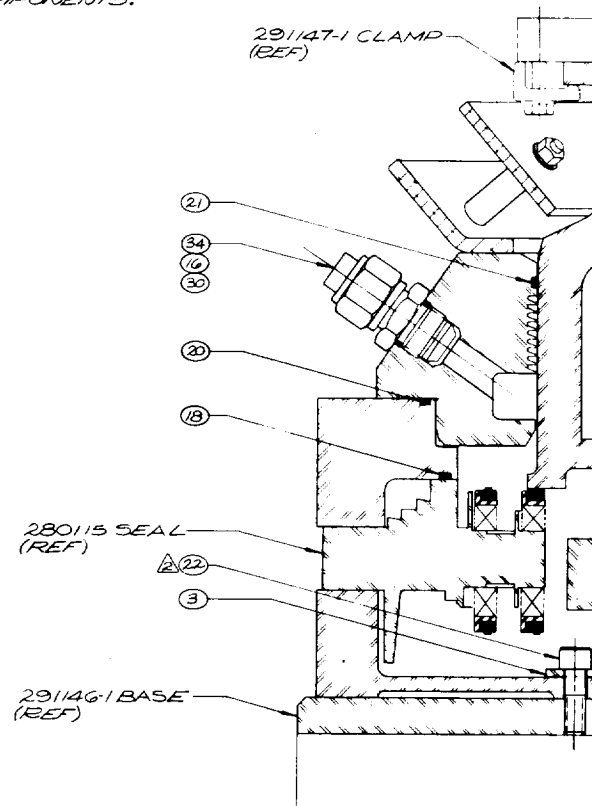
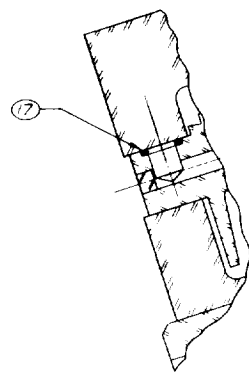
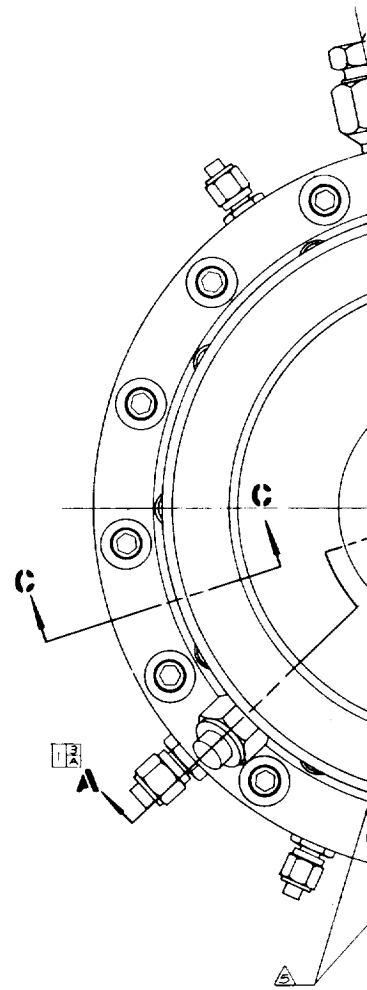




Figure 15 (Sheet 1 of 2)  
Effective Diameter Tester  
Page 35

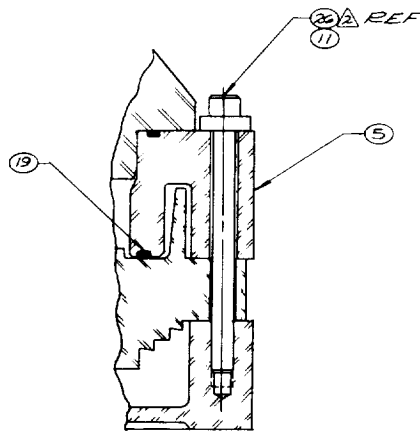
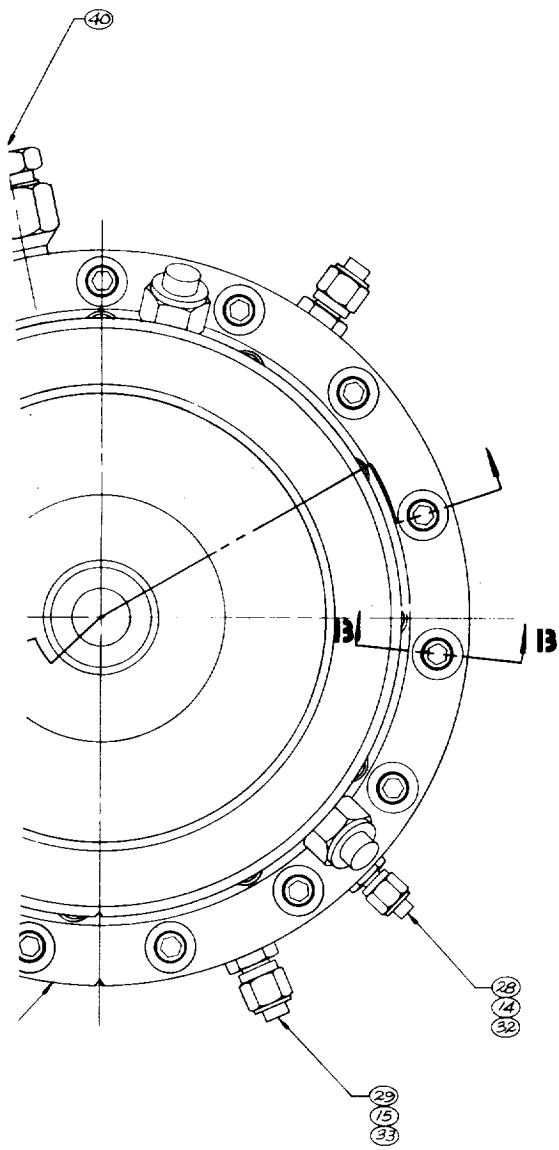




SECTION C-C



2



SECTION B-B

|         |        |        |
|---------|--------|--------|
| 05824   | E      | 291530 |
| 7/15/61 | 2 of 2 |        |

Figure 15 (Sheet 2 of 2)  
Effective Diameter Tester



provides the capability of defining the "effective diameter" as a function of applied fluid pressure and bellows compression, using gaseous nitrogen as a pressure fluid for static loading at room temperature.

#### (4) Test Activity and Results

"Effective diameter" checks were made on the primary liquid oxygen seal bellows of the oxidizer turbine seal assembly P/N 280115, S/N 023. The testing was conducted for two values of installed bellows compression (0.093 and 0.123 inch). The results are shown in Figures 16 through 19, where bellows effective diameter and seal overbalance values are a function of fluid pressure applied externally to the seal. Computations of this data were based upon the formulas shown on Pages 30 and 31 of this report. For comparison, the corresponding values supplied by Sealol are also shown. The results indicate that "effective diameter" and seal face overbalance are highly affected by a variation of fluid pressure acting on the bellows. For 500 psi pressure variation, the "effective diameter" changes as much as 0.110-in.

#### 2. Test Activity Conclusions

Analysis of the foregoing test development results was supported by theoretical work. The interaction and combination of all effects contributing to leakage is extremely complicated; available theories generally treat the subject by individual phenomenon and idealized conditions. However, a calculation of film thickness and leakage rates, based upon the theory of surface variance, indicates an interesting correlation to the actual liquid oxygen leakage experienced in the tests. This method is described in Appendix B.

In conventional dynamic seal theories and principles, upon which the subject seal design was based, tight dimensional control and precision sizing are strong functions in providing optimum seal performance. However, these are successful only to a point; and, if we consider dimensional proportions of a seal, the margin of possible improvement narrows drastically with increase of the sealing diameter. Despite all efforts toward dimensional perfection in manufacturing, the likelihood of retaining a theoretically perfect seal geometry during assembly and operation is rather small. Distortion of the seal elements may be induced by clamping effects, pressure, and thermal gradients. The seal face load, which directly affects wear and leakage rate, requires a precise hydraulic balance. However, the hydraulic balance is subject to considerable variance caused by the changes in effective diameter of the bellows as a function of pressure and possibly temperature. Pressure and temperature variations on the bellows also influence, to some degree, its spring force and thereby, the initial mechanical load on the seal face. The heat generation at the seal face caused by friction, which in all likelihood brings about a phase change in the liquid oxygen, is another contributing cause to the unpredictable pressure profile that exists at the seal face. Various theories are possible to derive from the test observations; however, the information gathered appears insufficient to account for all interacting phenomenon of a rubbing contact dynamic seal of relatively large proportions.

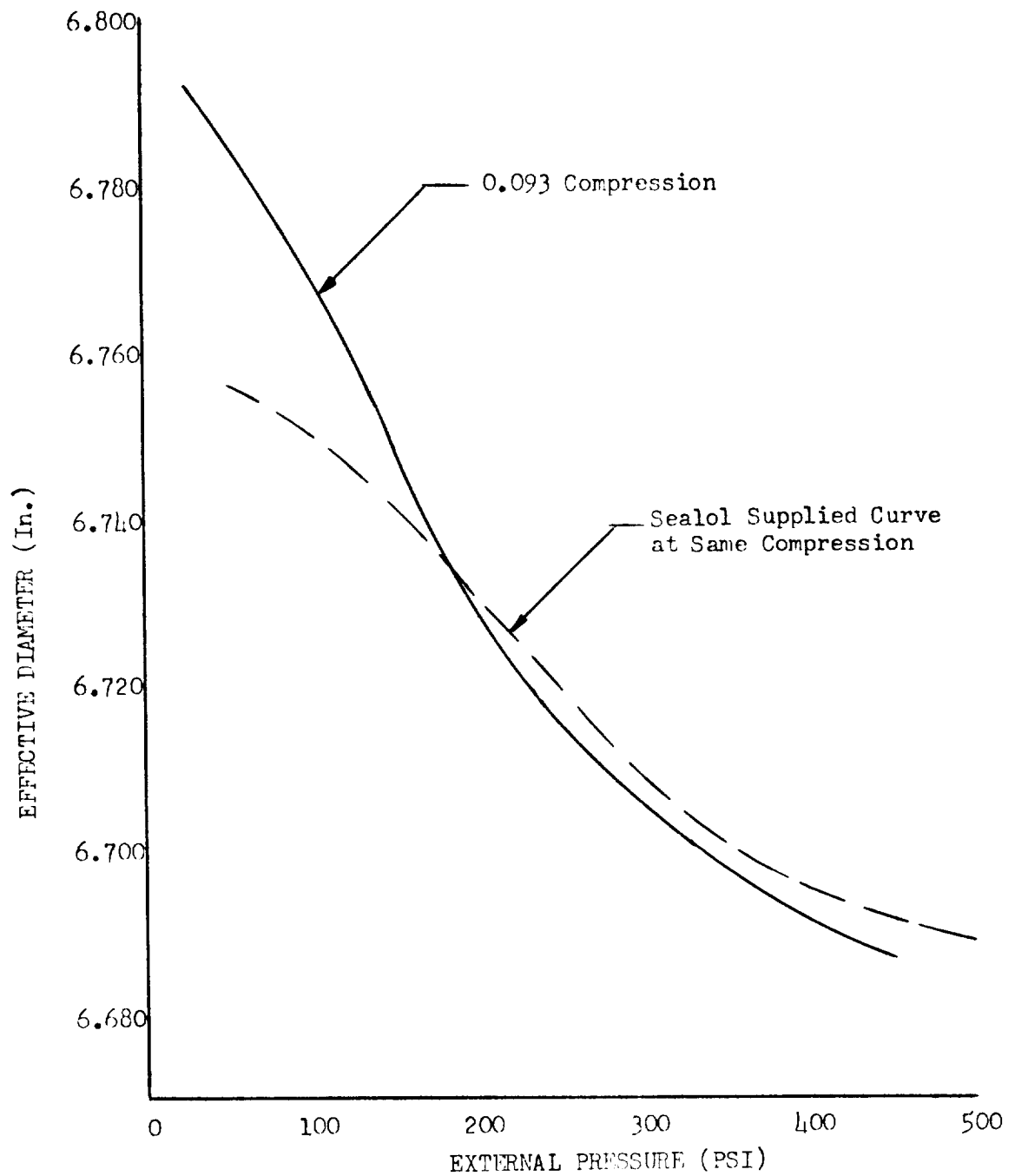


Figure 16  
Effective Diameter Vs External Pressure  
Page 38

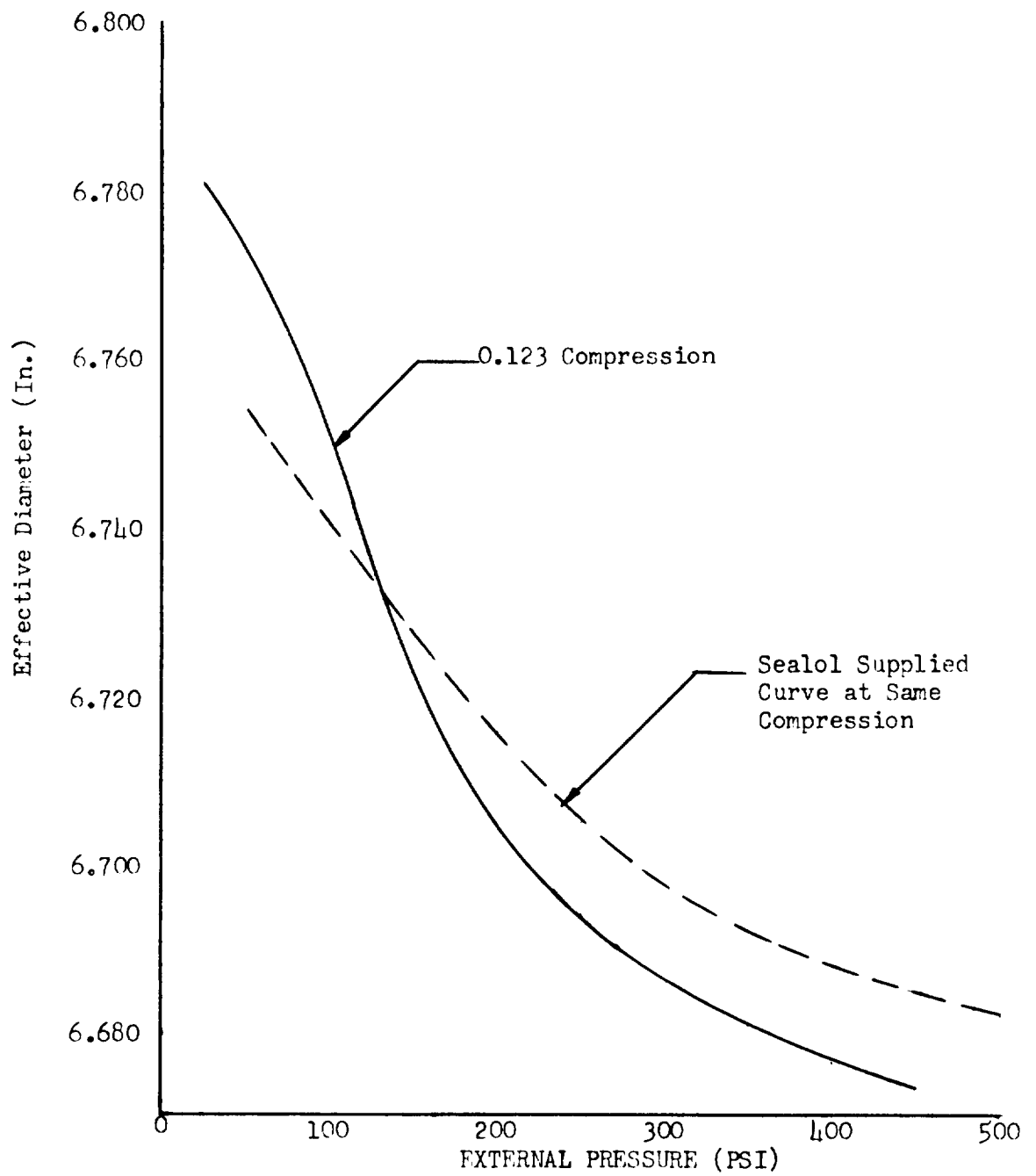


Figure 17  
Effective Diameter Vs External Pressure  
Page 39

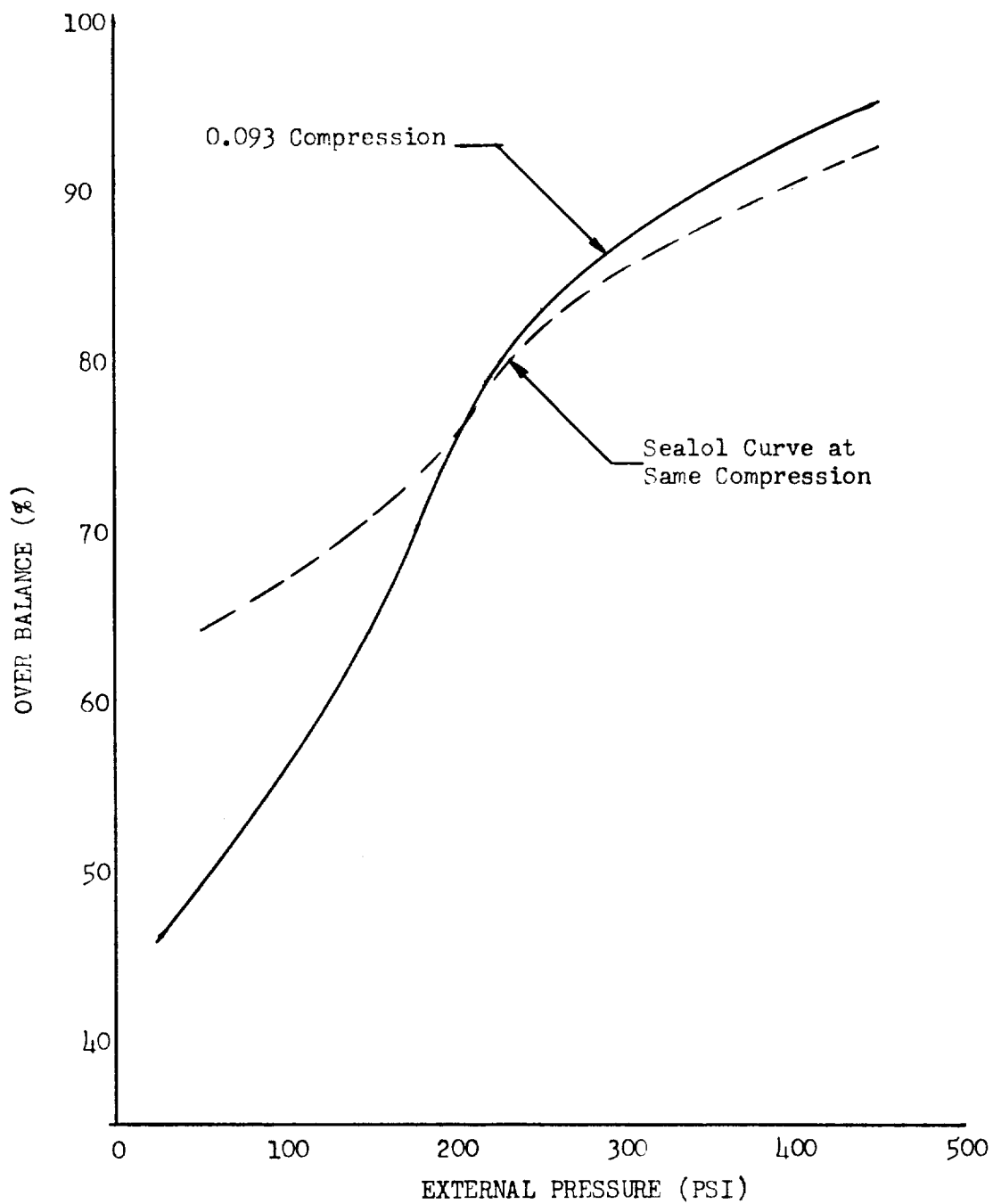


Figure 18  
Over Balance Vs External Pressure  
Page 40

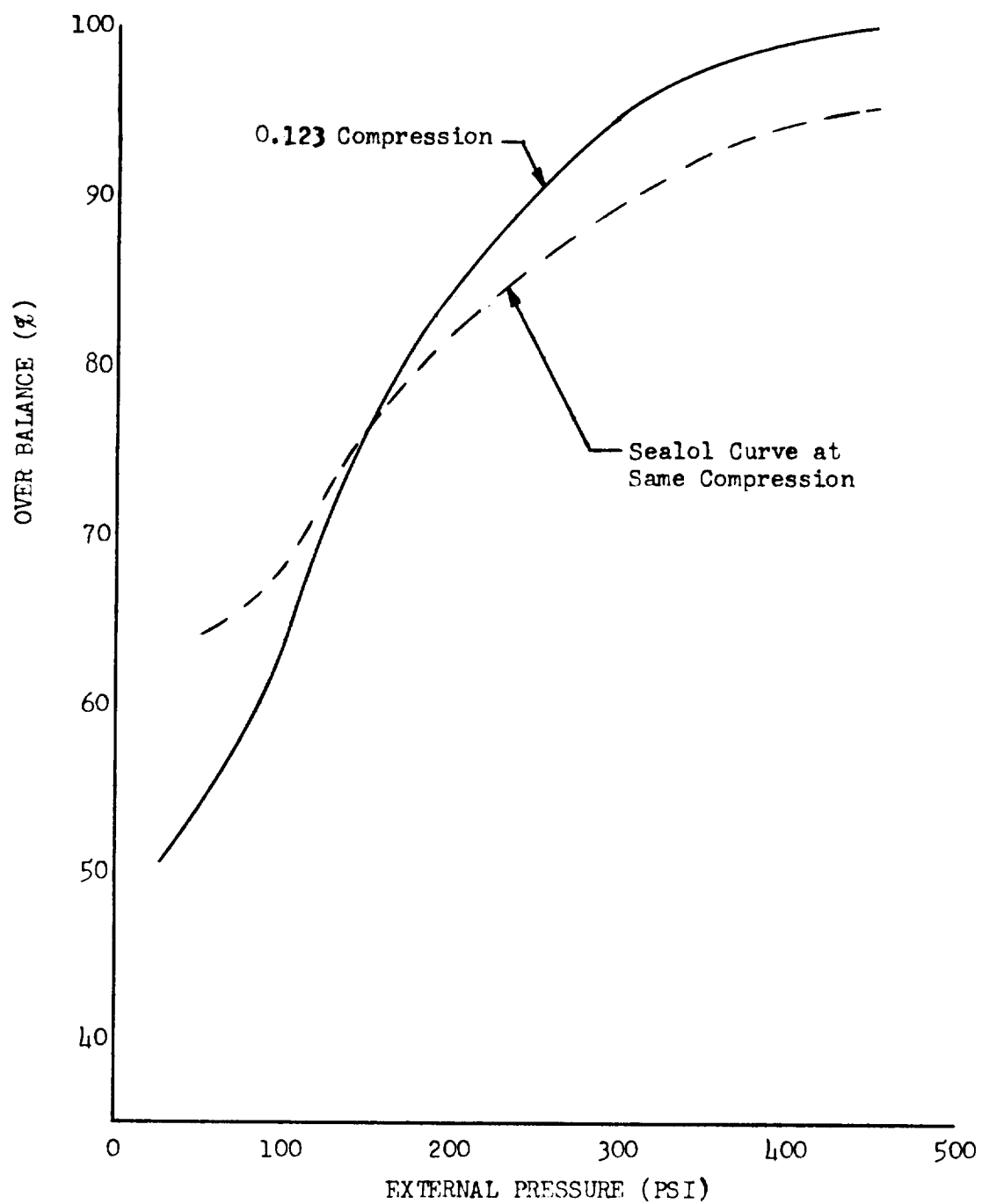


Figure 19  
Over Balance Vs External Pressure  
Page 41

The test development investigation of leakage causes produced relatively small improvement results in the areas investigated, with one important exception. Enlargement of the vent passages reduced the liquid oxygen flow across the primary seal face from  $1.6 \times 10^6$  scc/min (56.5 SCFM) to approximately 800,000 scc/min (28.25 SCFM), with the back pressure in the primary seal vent line never exceeding 3 psig.

In connection with the project requirement, the test results bring to light the severe lag of rubbing contact dynamic seal technology behind the requirements of existing turbomachinery and propulsion systems. A seal technology research activity, considerably broader than what is possible within the framework of this project oriented program, is recommended to alleviate the shortcoming. To satisfy the immediate project needs, a re-evaluation of the requirements as well as the hardware development potential appears in order. This includes consideration of a system modification which may provide the desired results in other ways than precise, rubbing contact "Zero Gap" seal faces.

#### D. MODIFICATION OF THE SEAL SYSTEM FOR TURBOPUMP USE

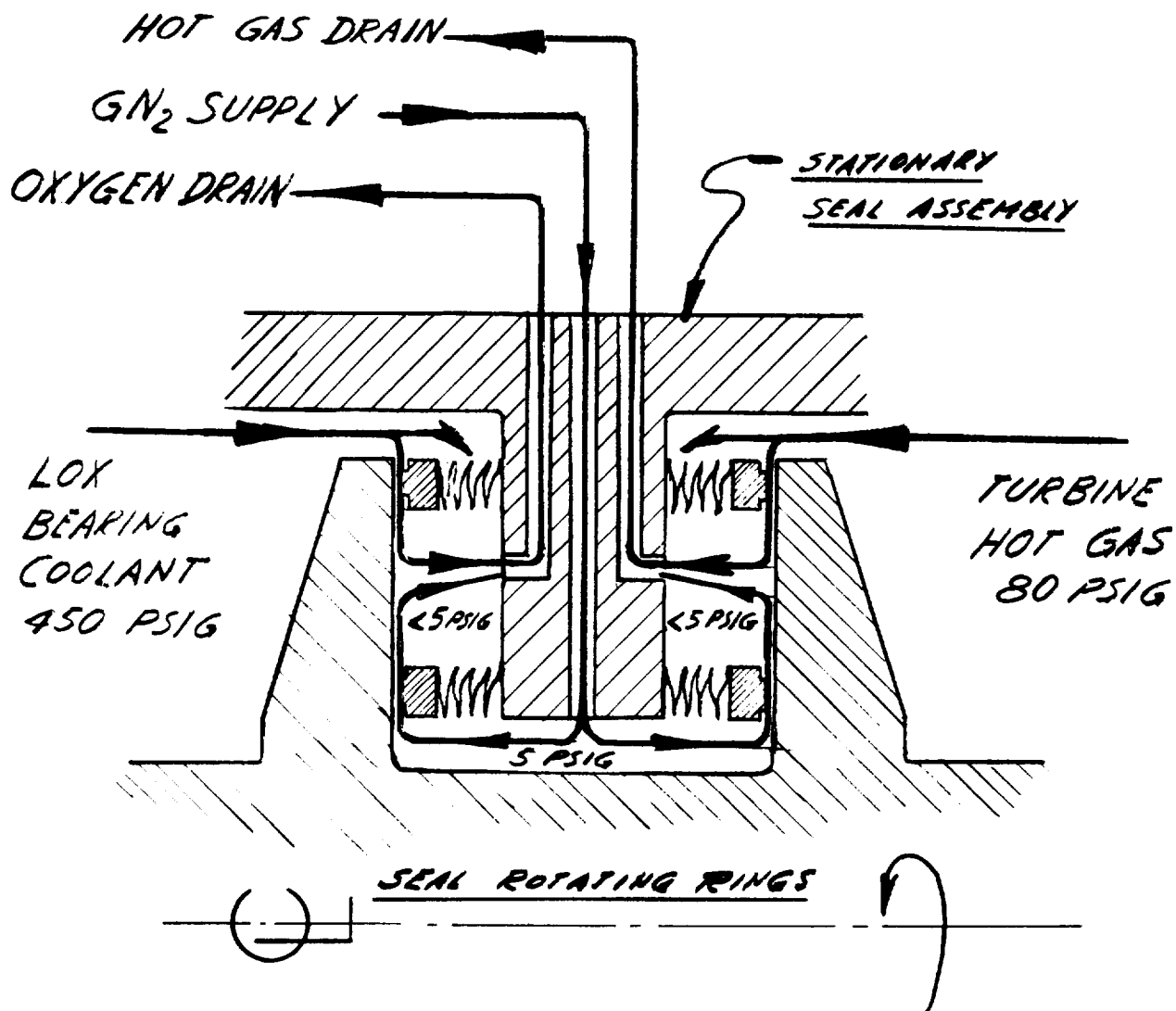
##### 1. Concept and Design Philosophy

In evaluating the degree of seal performance that was accomplished by development through Phase II of this program, it was evident that there was still much improving to be done to achieve the established goal and the performance necessary for M-1 oxidizer turbopump application. Timely accomplishment of this by pursuing development along the same lines was impractical. Consequently, a modification of the seal system was devised by introducing a continuous gaseous nitrogen purge in the seal neutral cavity. This technique restored both the effectiveness of the seal system and provided the means to positively prevent the mixing of the hot gas turbine gas with liquid oxygen. The purge pressure is maintained at 5 psig which is higher than cavity pressures under typical primary leakages. Minimizing the pressure buildup between the respective primary and secondary seals was accomplished by enlarging the vent passages from these cavities. Figure 20 is a schematic illustration of the purge system.

##### 2. Seal Hardware Modification

Implementation of the above described purge technique was predicated upon enlarging the vent passages of existing seal hardware. The original venting consisted of three 0.370-in. inside diameter lines: one connecting to the liquid oxygen cavity between the primary and secondary seal face; one to the hot gas cavity between its respective primary and secondary seal face; and one connecting to the annulus between the secondary liquid oxygen seal and the secondary hot gas seal. To this, twelve 1/2 in. diameter passages were added for liquid oxygen and six 3/8 in. diameter passages for hot gas. Also, provisions for six additional 3/8 in. passages to the "neutral" cavity were provided; however, only one additional 3/8 in. passage was used for supplying the continuous gaseous nitrogen purge to the cavity between the liquid oxygen secondary seal and the hot

SCHEMATIC DIAGRAM  
MODIFIED SEAL SYSTEM.



TYPICAL FLOW RATE OF  
GASEOUS NITROGEN PURGE:  
 $< 0.01 \text{ LB/SEC.}$

Figure 20

gas secondary seal. Figure 21 shows the location of the respective passages in the seal.

E. APPLICATION OF THE MODIFIED SEAL SYSTEM IN THE M-1 MODEL I  
OXIDIZER TURBOPUMP

1. Installation of the Modified Seal System

The drainage of oxygen leakage across the primary liquid oxygen seal is routed through twelve 1/2 in. diameter holes to the outside of the seal flange; there it is collected in an annular chamber and then piped through twelve 5/8 in. size tubings to a facility disposal manifold some distance away from the turbopump. Figure 22 illustrates the mechanical arrangement of the flow passages.

Hot gas leakage past the primary hot gas seal is channeled through the seal flange via six 3/8 in. diameter passages. The seal flange is provided with appropriate tube fitting connections and the leakage flow is piped to a disposal manifold by six 1/2 in. size tubings (See Figure 23).

Figure 24 shows the supply routing of the continuous gaseous nitrogen purge. This maintains a pressure of 5 psig gaseous nitrogen in the "neutral cavity" of the seal assembly. Adequate drainage lines for liquid oxygen and hot gas from the cavities between the respective primary and secondary seals assure that the back pressure in these cavities is less than 5 psig. Therefore, neither liquid oxygen nor hot gas can pass the secondary seals and enter the "neutral cavity." However, there is some flow (washing action) of gaseous nitrogen from the neutral cavity past the secondary liquid oxygen seal and the secondary hot gas seal from where it is evacuated through either the oxygen drain lines or the hot gas drain lines as a mixture with the respective medium.

The use of many relatively small size lines for piping the leakage from the seal to the outside of the turbopump was a development expediency utilizing existing hardware.

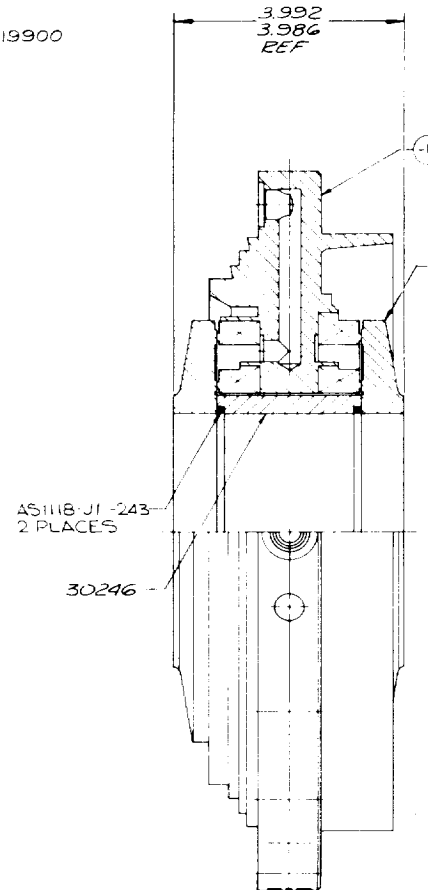
2. Performance During Turbopump Testing

The M-1 liquid oxygen turbopump turbine seal, using a low pressure gaseous nitrogen purge to prevent the mixing of cryogenic bearing coolant with the hot, hydrogen-rich turbine gas, was tested in the M-1 oxidizer turbopump assembly (S/N 001, Buildup 2).

Fourteen turbopump tests were run and 148 sec operating time was accumulated. The subject seal performed without failure. The measured gaseous nitrogen purge pressure was varied between 1.4 to 7.4 psig during the test runs. The gauge pressure in the primary seal vents for bearing coolant and hot gas, respectively, was zero at all times. This is a positive indication that mixing of the cryogenic bearing coolant with the turbine hot gas was reliably prevented. However, the cryogenic bearing coolant for this turbopump

NOTES:

1. REMOVE ALL BURRS AND SHARP EDGES EQUIV TO .005/.015 R UNLESS OTHERWISE NOTED.
2. INTERPRET DRAWING PER STANDARDS PRESCRIBED IN MIL-D-70327.
3. CLASSIFICATION OF CHARACTERISTICS PER MIL-W-9411 DENOTED BY (C) (CRITICAL), (M) (MAJOR), AND NO SYMBOL (MINOR).
4. SURFACE FINISH TO BE 125 UNLESS OTHERWISE NOTED.
5. MARK PER ASD5215C WITH "HG" AT PORTS ON 18°, 42°, 66°, 90°, 138°, & 162° FROM DATUM -A-.
6. MARK PER ASD5215C WITH "N" AT PORTS ON 186°, 210°, 270°, 294°, 318°, & 342° FROM DATUM -A-.
7. THE VENDOR SHALL SUPPLY WITH EACH SEAL DELIVERED TO AGC, THE BELLOWS SPRING RATES, FREE LENGTH, & EFFECTIVE DIA CURVES FROM ACTUAL TEST DATA FOR EACH SEAL SUBASSY.
8. REMOVED
9. CLEAN PER MSFC SPEC-144, TYPE III, CLASS I, FOR LIQUID OXYGEN SERVICE. ASSEMBLED UNIT TO BE MAINTAINED AT THIS LEVEL OF CLEANLINESS.
10. PRESERVE AND PACKAGE PER MSFC DWG NO. 10419900 FOR LIQUID OXYGEN SYSTEMS.
11. ABBREVIATIONS NOT COVERED BY MIL-STD-12:  
HG - HOT GAS  
N - NEUTRAL



MARK  
WITH  
& SEE



| REFUGEE |                 |              |         |
|---------|-----------------|--------------|---------|
| NO      | NAME            | REGISTRATION | DATE    |
| A       | SEE INCORP ADON |              | 10-1-68 |
| B       | SEE B ENG DCN   |              | 9-15-68 |

3

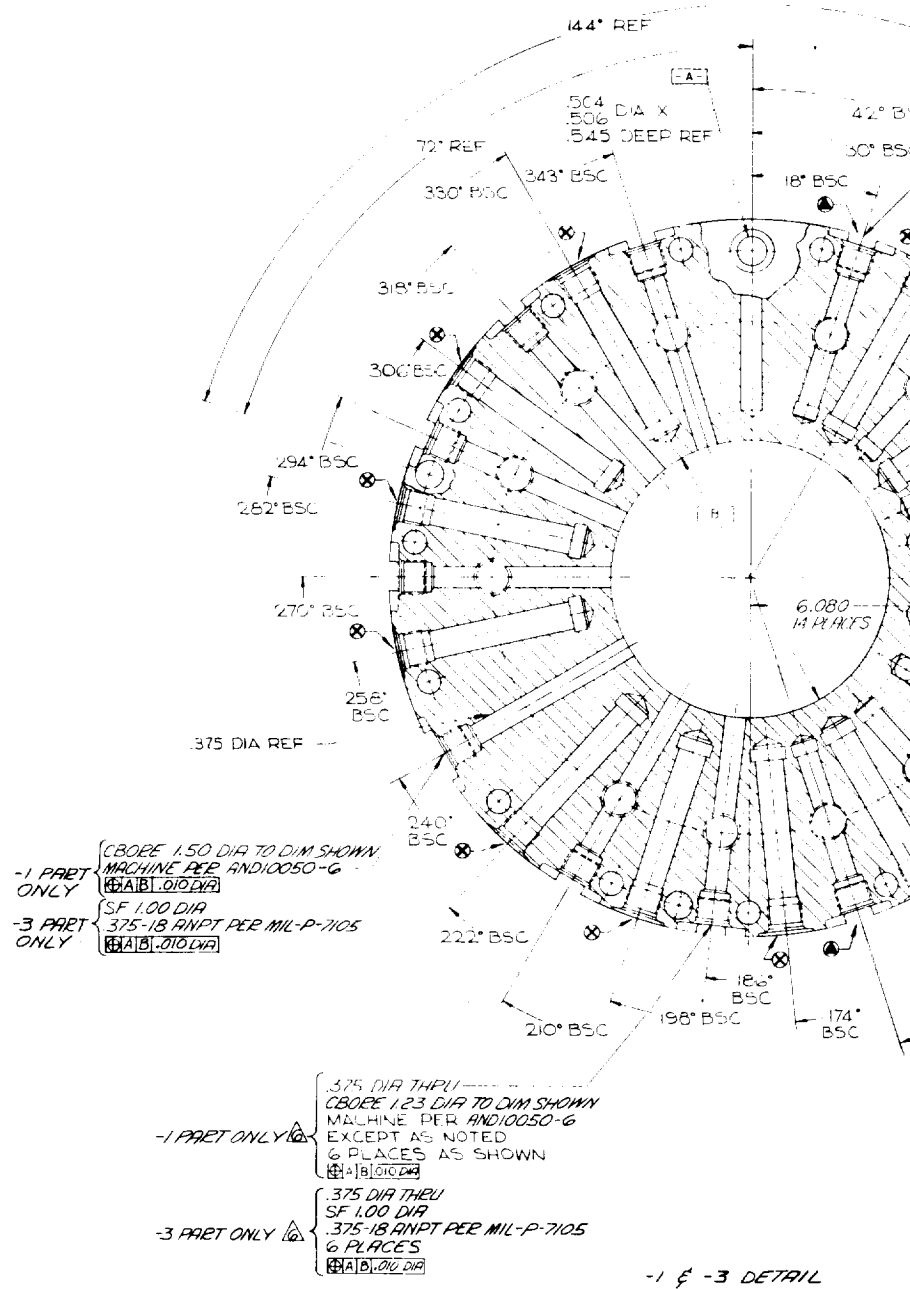
## ASSEMBLY

[illegible]

Page 45



SEE SHT 1 FOR G/N.

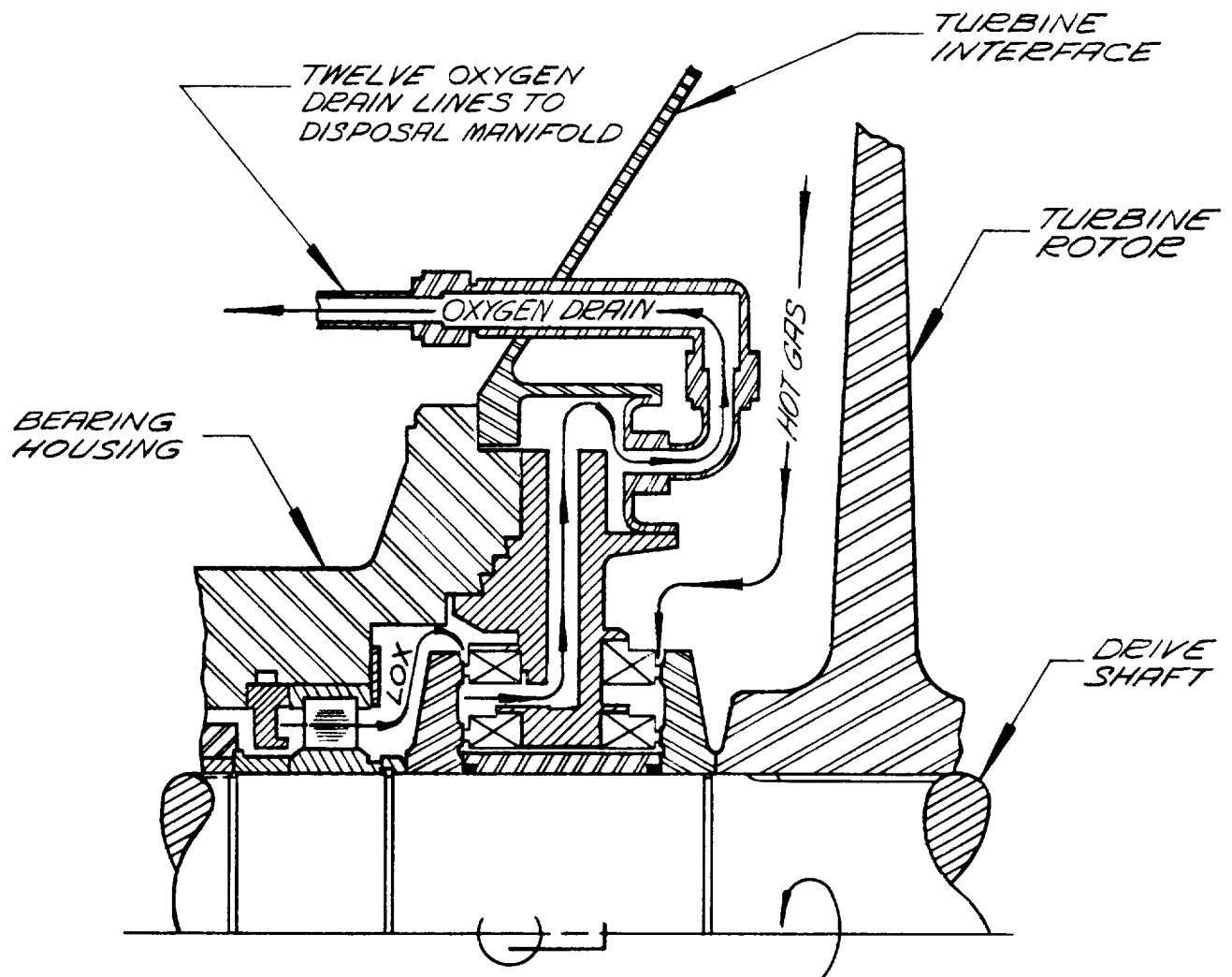








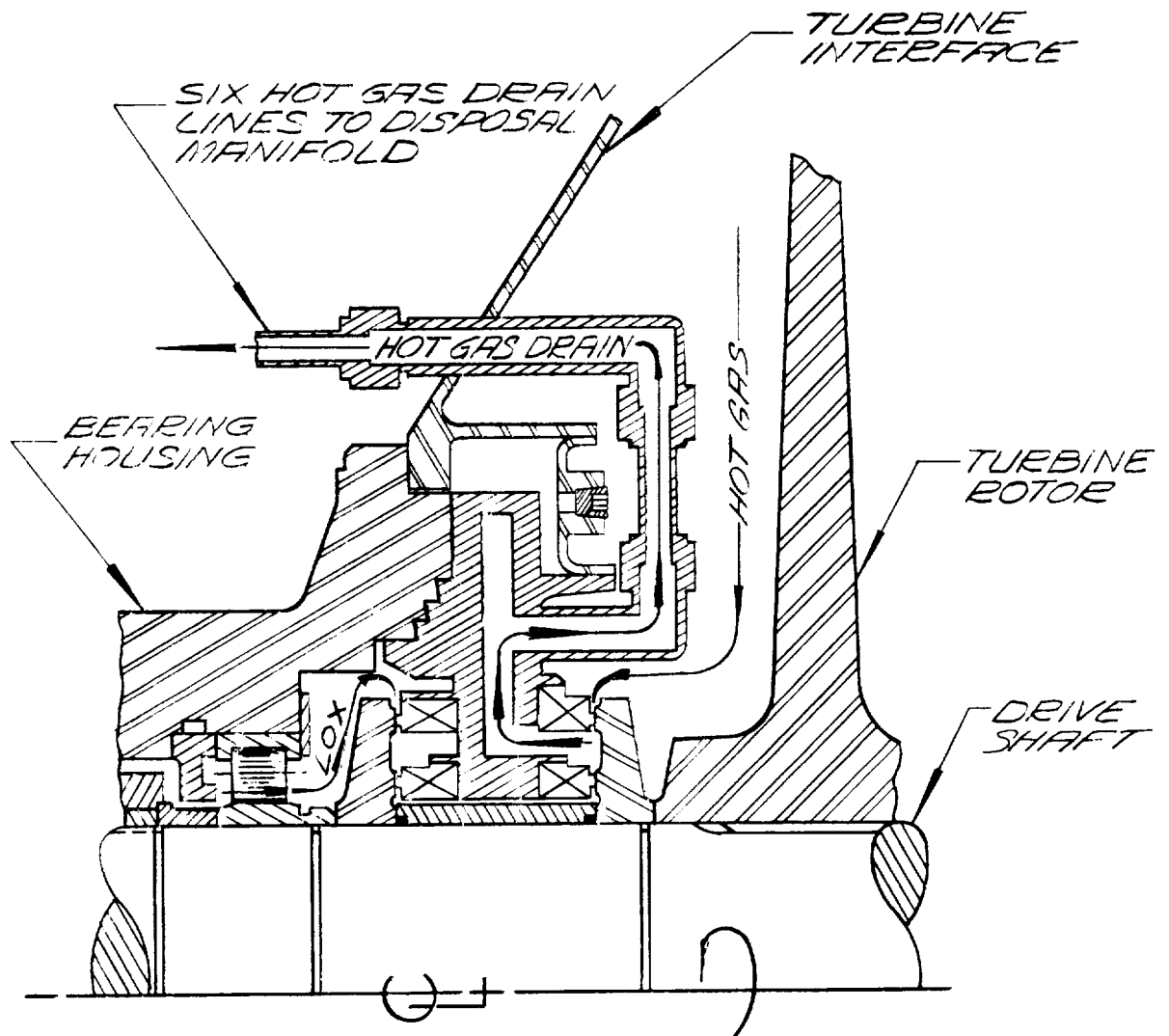
# MODIFIED SEAL SYSTEM (OXYGEN DRAIN)



(SEE FIG. 23 FOR HOT GAS DRAIN  
& FIG. 24 FOR GN<sub>2</sub> PURGE)

Figure 22

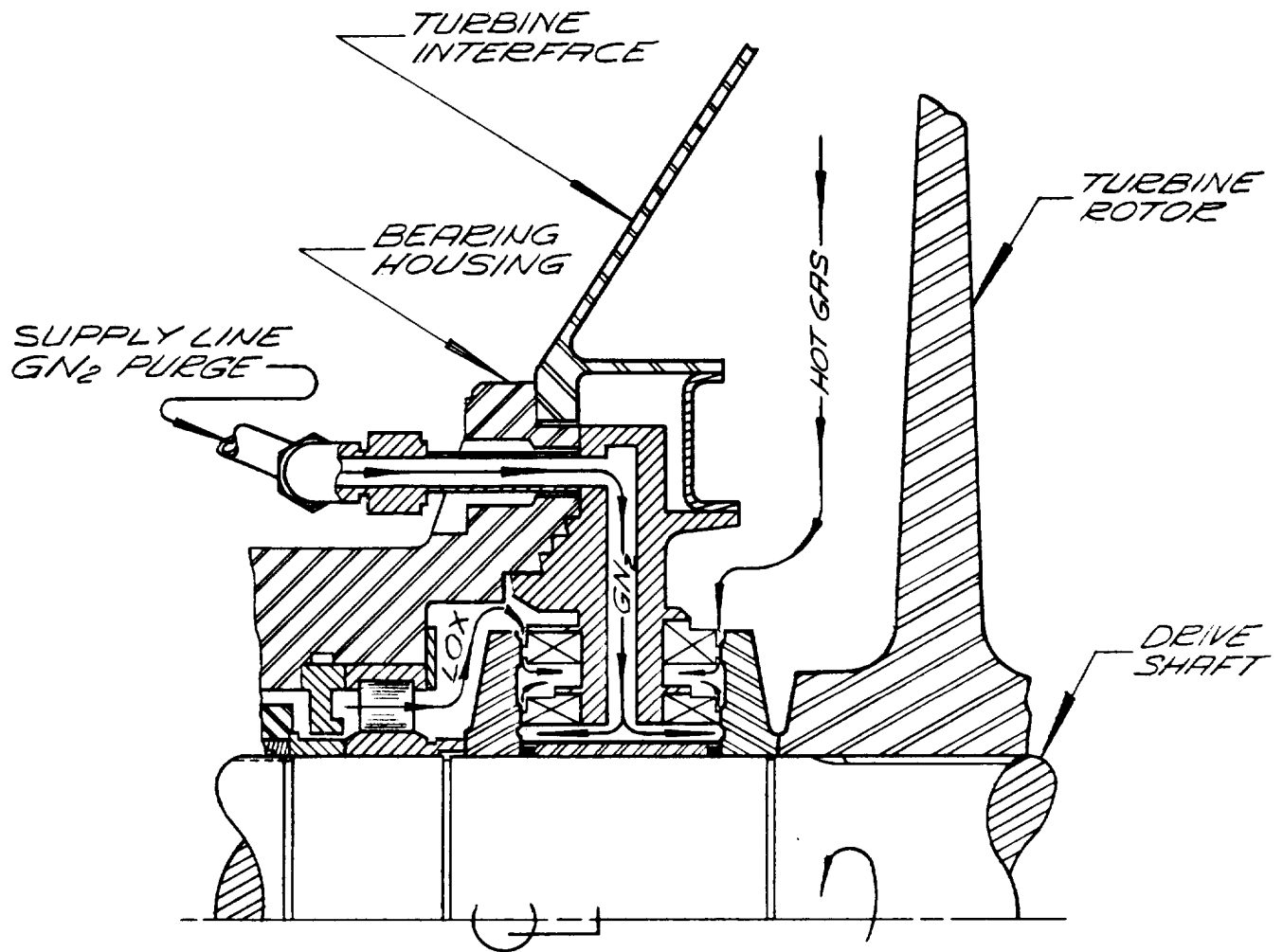
# MODIFIED SEAL SYSTEM (HOT GAS DRAIN)



(SEE FIG. 22 FOR OXYGEN DRAIN  
& FIG. 24 FOR  $GN_2$  PURGE)

Figure 23

*MODIFIED SEAL SYSTEM  
(GN<sub>2</sub> PURGE SUPPLY)*



*(SEE FIG. 22 FOR OXYGEN  
DRAIN & FIG. 23 FOR HOT  
GAS DRAIN)*

Figure 24

test series was liquid nitrogen and not liquid oxygen. No measurements of purge fluid flow rate were taken, but calculations indicate this to be less than 0.01 lb/sec.

Pre-test static leakage was checked by applying 50 psig nitrogen gas without having the purge connected to the "neutral cavity." The leakage was 60 cc/min, across the primary liquid oxygen seal and 90 cc/min across the primary secondary seal. There was no static leakage across either of the secondary seals.

#### IV. CONCLUSIONS AND RECOMMENDATIONS

The problem solution to positively prevent the mixing of hydrogen-rich hot turbine gas with liquid oxygen was provided by the introduction of nitrogen gas serving as a neutral barrier between the potentially explosive media. This seal system was installed in the M-1 Model I liquid oxygen turbopump and it was successfully operated.

The initial program attempt to achieve the stringent leakage requirement through a process of development to perfect a multi-element bellows face seal was abrogated after it became apparent that the necessary degree of perfection might not be obtainable within the time limit and mileposts established for the turbopump. Extrapolation of normal seal design criteria as derived from smaller seals does not appear to result in satisfactory large seals. In particular, the rigidity of the carbon retainer is inadequate in large seals to maintain low leakage at high pressure differentials.

By changing the solution approach and introducing a low pressure (5 psig) gaseous nitrogen purge to the seal's neutral cavity, a practical problem solution was provided and completely satisfied the project requirement.

### BIBLIOGRAPHY

1. G. W. Melnikov, M-1 Liquid Oxygen Primary Seal Analysis, Two Phase Flow, AGC Report TTR No. 001, 11 September 1964.
2. J. G. Stern, M-1 Liquid Oxygen Rotary Shaft Seal Theory and Criteria of Design, Part I, AGC Report, M-1 TPA No. 0001, 25 September 1964.



## APPENDICES



APPENDIX A

-

NOMENCLATURE



## APPENDIX A

### NOMENCLATURE

|            |   |   |
|------------|---|---|
| $A_A$      | = | Exposed Hydraulic Annulus Area, In. <sup>2</sup>      |
| $A_F$      | = | Total Seal Face Area, In. <sup>2</sup>                |
| $A_P$      | = | Fixture Piston Area, In. <sup>2</sup>                 |
| $D_E$      | = | Bellows Effective Dia., In.                           |
| $D_P$      | = | Fixture Piston Diameter, In.                          |
| $F$        | = | Total Axial Load on Seal Face, lb.                    |
| $P$        | = | Fluid Pressure on Bellows, Psig                       |
| $\Delta P$ | = | Change in Pressure, Psi                               |
| $\rho$     | = | Fluid Specific Weight, lb/in. <sup>3</sup>            |
| $C$        | = | Constant  |
| $g$        | = | Gravitational Acceleration = 386-in./sec <sup>2</sup> |
| $r_o$      | = | Seal Face Outside Dia. $\div$ 2, in.                  |
| $r_i$      | = | Seal Face Inside Dia. $\div$ 2, in.                   |
| $r_e$      | = | Bellows Effective Dia. $\div$ 2, in.                  |
| $A$        | = | Area, in. <sup>2</sup>                                |
| scc/min    | = | Standard Cubic Centimeter Per Minute                  |
| SCFM       | = | Standard Cubic Feet Per Minute                        |



APPENDIX B

ANALYTICAL TREATMENT OF SEAL LEAKAGE

BY

T. PASTERNAK



## APPENDIX B

### ANALYTICAL TREATMENT OF SEAL LEAKAGE

#### I. INTRODUCTION

The results from testing the liquid oxygen seal at operating conditions showed that the leakage rates were greatly in excess of those predicted by the seal designers (i.e., some 800,000 cc/min compared to 30,000 maximum expected).

In this case, the seals were designed by the common practice of extrapolating information obtained from earlier experience by the seal manufacturer. Outside of the mechanical features of the seal such as bellows design, method of carbon mounting, choice of materials, etc. which are stock-in-trade items of the seal manufacturer, the most important parameter by which the designer hopes to control leakage rates and life of the seal, is so called "overbalance". Broadly speaking, overbalance determines the amount of hydraulic load applied to the back of the seal in order to keep the carbon against the rotating ring with enough force to minimize the leakage, yet not so large as to cause rapid wear of seal elements.

The term overbalance is in itself somewhat of a misnomer, since it implies a lack of balance. In actuality the forces acting on the seal from both sides are always equal and therefore always in balance, as explained in Section II.

A selection of particular value of overbalance is related to the expectation of a particular profile on the sealing face, e.g., Overbalance = .52 implies a linear pressure drop from outer to inner seal diameter; Overbalance = 1.0 implies a constant pressure from outer to inner seal diameter. In both cases a uniform and constant pressure profile around circumference is implied.

The current state-of-the-art, when applied to the design of the liquid oxygen seal, apparently dictated the choice of 0.92 overbalance on the basis of previous experience of the seal designers. However, it should be pointed out that opinions varied between experts as to correct choice with values varying from 0.66 to 0.92.

The weakness of this empirical approach is that the film conditions vary greatly depending upon the application and currently there are no means of estimating leakage rates as a function of overbalance as applied to design. Clearly, in order to eliminate the trial and error approach, a mathematical model describing the film conditions between the faces as a function of overbalance, seal geometry, sealing surface conditions, fluid properties, operational conditions and then relating these to leakage rates, is needed. A number of such models, based upon vibration, surface tension, or surface waviness, are described in seal literature although none, to the writers knowledge, combines all effects in a single model.

To list some - Reference 1 describes the effect of axial vibration on the pressure between the sealing faces and in Reference 2 the effects of surface tension on the film thickness and leakage rates are examined. In Reference 3 the effects of seal surface waviness on the pressure profile and leakage rates are described.

The hydrodynamic theory developed in Reference 3 was selected as a basis for the attempted analytical correlation. It was recognized that this the mathematical model was not necessarily complete or even correct, since however, it contained relationships between the important design and performance parameters (i.e., leakage, overbalance, seal size, pressure, rpm, fluid properties, (viscosity) and seal surface conditions) and the results were in the form which could be used

with very minor rearrangements. It was felt that this theory may serve as a useful opening, to which refinements and additions would be made in the future. The seal development program was, however, discontinued and therefore this report contains only the description of the method and initial results. It should be pointed out, however, that the leakage rates as calculated are surprisingly close to those reported in tests, and therefore the approach may warrant further investigation. In addition, the writer believes that (at least in a qualitative sense) it is a step forward in an attempt to elucidate the mechanism of dynamic sealing.

## II. CONCEPT OF OVERBALANCE AND ITS INADEQUACY AS PRINCIPAL DESIGN PARAMETERS

It was already pointed out that the current state-of-the-art of seal design is such that the designer must make a purely empirical selection of the principal design parameter (i.e. "overbalance") which then controls the hydraulic loading of the seal and will hopefully result in low leakage and satisfactory seal life. The concept of "overbalance" is obtained from the following basic relationships:

Consider Figure B-1 where:

- $r_o$  outside radius of seal
- $r_i$  inside radius of seal
- $r_e$  effective diameter of bellows (i.e., O.D. of equivalent seal piston)
- $P_o$  sealant pressure
- $P_i$  vent seal pressure (assumed zero)
- $F_s$  spring force of the bellows (negligible comparing to hydraulic forces and is neglected)
- $P_F$  local pressure on the front face at radius  $r$ .
- $P_B$  local pressure on the back of the seal at radius  $r$ .

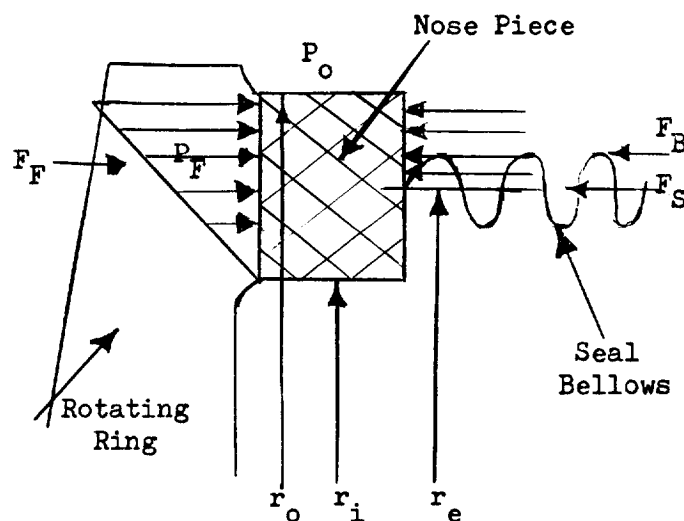


Figure B-1

Since seal is in equilibrium under the action of all forces

$$F_B + F_S = F_F \text{ and } F_B \approx F_F \text{ approximately} \quad (1)$$

In order to obtain the value of both forces in terms of known pressure  $P_o$  and seal dimensions equation (1) must be put in the differential form.

$$\int_{r_o}^{r_e} \int_{r_o}^{2\pi} P_B \cdot r \cdot dr \cdot d\theta = \int_{r_o}^{r_e} \int_{r_o}^{2\pi} P_F \cdot r \cdot dr \cdot d\theta \quad (2)$$

In order to integrate both sides of the Equation (2) it is necessary to determine the form of pressure profile on both back and front faces of the seal both as a function of radius ( $r$ ) and also of angle ( $\theta$ ).

For the back face pressure ( $P_B$ ) is assumed constant and equal to  $P_o$ , i.e.,  $P_B(r, \theta) = P_o$

$$\text{Therefore } F_B = \int_{r_o}^{r_e} \int_{r_o}^{2\pi} P_o \cdot r \cdot dr \cdot d\theta = \pi P_o (r_o^2 - r_e^2) \quad (3)$$

For the front face the matter is more complicated since the pressure profile is not known. Making a usual assumption that pressure  $P_f$  varies linearly between  $r_o$  and  $r_i$  and maintains the same profile around the circumference.

$$\begin{aligned} \text{i.e., } P_F(r, \theta) &= P_o \left[ \frac{r - r_i}{r_o - r_i} \right] \\ F_F &= P_o \left( \frac{2r_o + r_i}{r_o + r_i} \right) \times \left( \frac{r_o^2 - r_i^2}{3} \right) \\ &= K \pi P_o (r_o^2 - r_i^2) \end{aligned} \quad (4)$$

$$\text{for thin seal face where } \frac{r_o}{r_i} < 1.1 \quad K \approx .5$$

Combining equations (1), (3), and (4) results in

$$K = \frac{r_o^2 - r_e^2}{r_o^2 - r_i^2}$$

Expression for K in Equation (5) will be readily recognized as the "overbalance", a parameter commonly used in seal design terminology.

Its magnitude was shown to be approximately .5 if pressure profile was linear on the "sealing" face of the seal, and it can easily be shown that it will be progressively larger and may even exceed 1.0 if pressure is "bulging out" from linearity.

In present day seal design practice the value of overbalance is selected by the designer on the basis of his previous experience and this value is used in equation (5) to determine effective radius ( $r_e$ ) of the bellows for this particular application.

It appears that the empirical approach to the selection of overbalance is unsatisfactory at least with respect to making predictions of leakage rates and life in novel designs like liquid oxygen seal and that the designer must be furnished with better and more fundamental basis for the selection of K involving considerations of seal operational requirements (pressure and speed), sealing fluid properties, seal size ( $r_o$ ), and allowable leakage and minimum life requirements, if guess-work is to be eliminated from the seal design.

An attempt of resolving this problem in reverse is to determine the leakage as a function of K for the M-1 primary liquid oxygen seal on the basis of mathematics of hydraulic film between the wavy surfaces in relative rotary motion. This is described in Section III.

### III. LEAKAGE RATES VS OVERBALANCE CALCULATIONS BASED ON SURFACE WAVINESS THEORY

The method of calculation of leakage rates as a function of overbalance for the liquid oxygen primary seal was derived from the mathematical relationships described by F. A. Lyman and E. Saibel in the paper entitled "Leakage in Rotary Shaft Seals" and based upon the concept of hydrodynamic film development between wavy surfaces in relative motion. The derivation of the mathematical equations is shown by directly reproducing pertinent parts of the authors work using their terminology. These equations are then rewritten in terminology useful to the seal designer and are used to calculate leakage rates that would be expected in the liquid oxygen seal on the basis of this theory.

## A. DERIVATION OF BASIC EQUATIONS

(Derived in F. A. Lyman and E. Saibel report)

### Introduction

This paper presents some preliminary results of a theoretical investigation of leakage through a rotary shaft seal (Fig. 1). If the faces of the seal were perfectly flat and exactly parallel, in the absence of axial motion of the faces the leakage through the interfacial gap would be independent of the shaft speed and proportional to the pressure difference across the seal. The pressure in the gap would be of the order of the average of the inner and outer pressures. However, Jagger [1] and Denny [2] have noted that pressures considerably higher than this are developed in radial seals. Furthermore, the leakage rate was found to depend on shaft speed [2].

Theoretical investigations of the effect of axial vibration on the pressure developed in rotary shaft seals have been carried out by Iny and Cameron [3], Whiteman [4], and Nahavandi and Osterle [5]. In the present study, attention is concentrated on other possible causes for the dependence of pressure and leakage on the shaft speed:

1. Waviness of the faces, i.e. small continuous variations in the interfacial distance.
2. Shaft misalignment, causing nonparallel surfaces and/or wobble.

### Analysis

Reynolds' equation in polar coordinates ( $r, \phi, z$ ) for the flow of an incompressible fluid in the thin film be-

<sup>1</sup>This work was sponsored by the U.S. Naval Engineering Experiment Station, Annapolis, Maryland.

tween the stationary surface  $z = 0$  and the rotating surface  $z = h(r, \phi, t)$  is

$$r \frac{\partial}{\partial r} \left( h^3 r \frac{\partial p}{\partial r} \right) + \frac{\partial}{\partial \phi} \left( h^3 \frac{\partial p}{\partial \phi} \right) = 6\mu r^2 \left( \omega \frac{\partial h}{\partial \phi} + 2 \frac{\partial h}{\partial t} \right). \quad (1)$$

where  $r$  and  $\phi$  are the polar coordinates of a point

$t$  is time

$h$  is film thickness

$p$  is pressure

$\omega$  is angular velocity

and  $\mu$  is coefficient of viscosity

The rate of flow in the radial direction per unit of circumference is

$$q_r = \int_0^h v_r dz = - \frac{h^3}{12\mu} \frac{\partial p}{\partial r}, \quad (2)$$

so that the leakage through the seal can be found from (2) once the solution of (1) is known.

Equation (1) will be applied to the two cases mentioned above.

#### 1. Effect of Waviness in the Rotating Face

Suppose the waviness is on the surface of the rotating seal. Thus in a system of coordinates which rotates with angular velocity  $\omega$  (Fig. 2),  $h$  is independent of time, so if we let  $\theta = \phi - \omega t$ ,  $h = h(r, \theta)$  and (1) becomes

$$r \frac{\partial}{\partial r} \left( h^3 r \frac{\partial p}{\partial r} \right) + \frac{\partial}{\partial \theta} \left( h^3 \frac{\partial p}{\partial \theta} \right) = - 6\mu \omega r^2 \frac{\partial h}{\partial \theta} \quad (1.1)$$

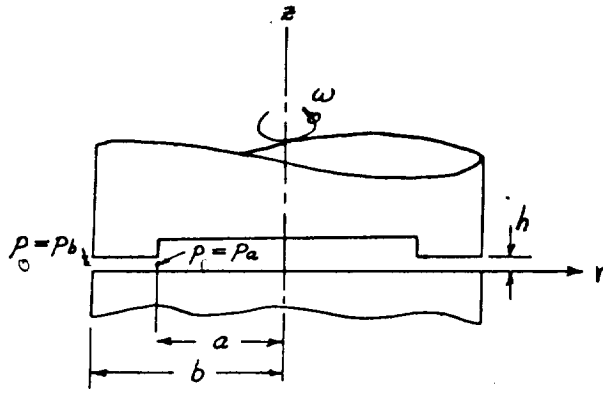


FIGURE 1. ROTARY SHAFT SEAL

Let the waviness be described by the function

$$h = h_0 (1 + \epsilon \cos \theta) \quad (1.2)$$

where  $0 < \epsilon < 1$ . An exact solution of (1.1) for  $h$  given by (1.2) has not been found. Here an approximate solution will be obtained by a perturbation method. It is assumed that  $\epsilon$  is small, and the pressure is expanded in powers of  $\epsilon$ :

$$p = p_0(r) + \epsilon p_1(r, \theta) + \epsilon^2 p_2(r, \theta) + \dots \quad (1.3)$$

After substituting (1.2) and (1.3) into (1.1) and setting the coefficient of each power of  $\epsilon$  equal to zero, we obtain the equations

$$\frac{d}{dr} \left( r \frac{dp_0}{dr} \right) = 0 \quad (1.4)$$

$$r \frac{\partial}{\partial r} \left( r \frac{\partial p_1}{\partial r} \right) + \frac{\partial^2 p_1}{\partial \theta^2} = \frac{6\mu\omega}{h_0^2} r^2 \sin \theta \quad (1.5)$$

$$r \frac{\partial}{\partial r} \left( r \frac{\partial p_2}{\partial r} \right) + \frac{\partial^2 p_2}{\partial \theta^2} = -3 \cos \theta r \frac{\partial}{\partial r} \left( r \frac{\partial p_1}{\partial r} \right) - 3 \frac{\partial}{\partial \theta} \left( \cos \theta \frac{\partial p_1}{\partial \theta} \right) \quad (1.6)$$

The solution of (1.4) which satisfies the boundary conditions

$$\begin{aligned} p_0(a) &= p_a \\ p_0(b) &= p_b \end{aligned} \quad (1.7)$$

is

$$p_0 = A_0 \ln \frac{r}{a} + p_a \quad (1.8)$$

where

$$A_0 = \frac{p_b - p_a}{\ln \frac{b}{a}}$$

Equation (1.8) represents the pressure distribution in a

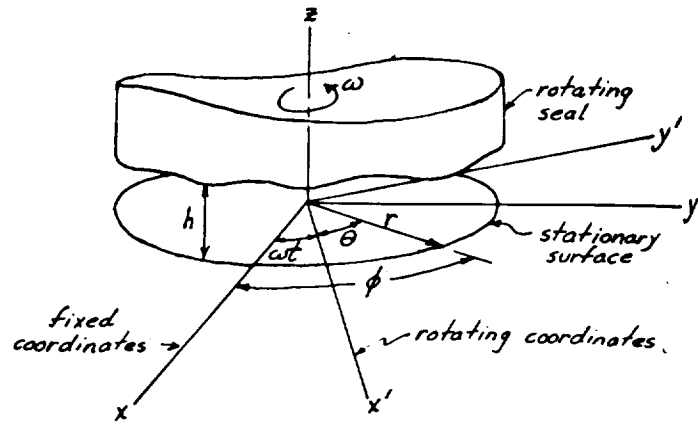


FIGURE 2. COORDINATE SYSTEMS

parallel surface seal, and this pressure is independent of  $\omega$ .

The solution of (1.5) which satisfies the boundary conditions

$$p_1(a, \theta) = p_1(b, \theta) = 0$$

is

$$p_1 = \frac{2\mu\omega}{h_0^2} (r^2 + A_1 r + B_1 r^{-1}) \sin \theta \quad (1.9)$$

where

$$\begin{aligned} A_1 &= -\frac{b^3 - a^3}{b^2 - a^2} \\ B_1 &= \frac{a^2 b^2 (b - a)}{b^2 - a^2} \end{aligned}$$

Since  $(r^2 + A_1 r + B_1 r^{-1}) \leq 0$  for  $a \leq r \leq b$ ,  $p_1 \geq 0$  for  $\pi \leq \theta \leq 2\pi$ , i.e. in the converging portion of the film. Since negative pressures are unrealistic,  $p_1$  will be assumed to be zero for  $0 \leq \theta \leq \pi$ .

The load contributed by  $p_1$  is

$$W_1 = \int_{\pi}^{2\pi} \int_a^b p_1 r dr d\theta = \frac{\mu\omega}{3h_0^2} (b-a)^3 \left( b + a + \frac{2ab}{b+a} \right) \quad (1.10)$$

In the absence of applied pressures,  $\epsilon W_1$  is the total load-carrying capacity of the seal, correct to the second order in  $\epsilon$ . If a log-log plot of  $h_0$  vs.  $W_1$  were made from (1.10), the result would be a straight line with slope  $-0.5$ . Log-log plots of Denny's experimental results ([2], Fig. 3) also appear as straight lines, but with slopes of about  $-0.2$  or  $-0.3$ .

The rate of flow through the seal in the radial direction is

$$Q = \int_0^{2\pi} q_r r d\theta \quad (1.11)$$

Writing  $Q = Q_0 + \epsilon Q_1 + \epsilon^2 Q_2 + \dots$ , from (2) we find

$$Q_0 = -\frac{1}{12\mu} \int_0^{2\pi} h_0^3 r \frac{\partial p_0}{\partial r} d\theta = -\frac{\pi h_0^3 A_0}{6\mu} \quad (1.12)$$

$$\begin{aligned} Q_1 &= -\frac{h_0^3}{12\mu} \int_0^{2\pi} \left( r \frac{\partial p_1}{\partial r} + 3 \cos \theta r \frac{dp_c}{dr} \right) d\theta \\ p_1 &\geq 0 \\ &= -\frac{h_0^3}{12\mu} \int_0^{2\pi} r \frac{\partial p_1}{\partial r} d\theta \\ p_1 &\geq 0 \\ &= \frac{\omega h_0}{3} (2r^2 + A_1 r - B_1 r^{-1}) \end{aligned} \quad (1.13)$$

The inward leakage rate for no pressure difference across the seal is  $-(Q_1)_{r=a}$  and is positive.

Substitution of (1.9) into (1.6) leads to the following equation for  $p_2$ :

$$r \frac{\partial}{\partial r} \left( r \frac{\partial p_2}{\partial r} \right) + \frac{\partial^2 p_2}{\partial \theta^2} = \frac{3\mu\omega}{h_0^2} (-2r^2 + A_1 r + B_1 r^{-1}) \sin 2\theta \quad (1.16)$$

The solution of (1.16) which satisfies the boundary conditions  $p_2(a, \theta) = p_2(b, \theta) = 0$  is

$$\begin{aligned} p_2 &= -\frac{3\mu\omega}{h_0^2} \left( \frac{1}{2} r^2 \ln r + \frac{A_1}{3} r + \frac{B_1}{3} r^{-1} + A_2 r^2 + B_2 r^{-2} \right) \times \sin 2\theta \\ &= -\frac{3\mu\omega}{h_0^2} f_2(r) \sin 2\theta \end{aligned} \quad (1.17)$$

where

$$A_2 = -\frac{1}{2} \frac{b^4 \ln b - a^4 \ln a}{b^4 - a^4} - \frac{A_1}{3} \frac{b^3 - a^3}{b^4 - a^4} - \frac{B_1}{3} \frac{b - a}{b^4 - a^4}$$

$$B_2 = \frac{1}{2} \frac{a^4 b^4 \ln b/a}{b^4 - a^4}$$

Since  $f_2(r) < 0$  for  $a < r < b$ ,  $p_2 > 0$  for  $0 < \theta < \pi/2$  and  $\pi < \theta < 3\pi/2$ .<sup>2</sup> Hence the second order term for the load capacity is

$$\begin{aligned} W_2 &= \int_0^{2\pi} \int_a^b p_2 r dr d\theta = -\frac{6\mu\omega}{h_0^2} \int_a^b r f_2(r) dr \\ p_2 &\geq 0 \\ &= -\frac{6\mu\omega}{h_0^2} \left[ -\frac{b^4 - a^4}{32} + \frac{A_1}{36} (b^3 - a^3) + \frac{B_1}{4} (b - a) + B_2 \ln \frac{b}{a} \right] \end{aligned} \quad (1.18)$$

The radial flow rate is

$$Q_2 = -\frac{h_0^3}{12\mu} \int_0^{2\pi} \left( r \frac{\partial p_2}{\partial r} + 3 \cos \theta r \frac{\partial p_1}{\partial r} + 3 \cos^2 \theta r \frac{\partial p_0}{\partial r} \right) d\theta \quad (1.19)$$

$p_1, p_2 \geq 0$

But

$$\int_0^{2\pi} \cos \theta r \frac{\partial p_1}{\partial r} d\theta = 0$$

$$p_1 \geq 0$$

$$\int_0^{2\pi} \cos^2 \theta r \frac{\partial p_0}{\partial r} d\theta = \pi A_0$$

$$\int_0^{2\pi} r \frac{\partial p_2}{\partial r} d\theta = -\frac{6\mu\omega}{h_0^2} r f_2'$$

$$p_2 \geq 0$$

Hence the second correction to the inward leakage rate is

$$\begin{aligned} L_2 = (-Q_2)_{r=a} &= -\frac{\omega h_0}{2} \left( \frac{a^2}{2} + a^2 \ln a + \frac{A_1}{3} a - \frac{B_1}{3} a^{-1} \right. \\ &\quad \left. + 2A_2 a^2 - 2B_2 a^{-2} \right) - \frac{\pi A_0 h_0^3}{4\mu} \end{aligned} \quad (1.20)$$

Note that  $W_2, L_2$  depend on  $\omega$  and  $h_0$  in the same manner as do  $W_1, L_1$ . If as above  $\epsilon = 10^{-5}$ , then  $\epsilon^2 W_2$  and  $\epsilon^2 L_2$  would be negligible compared to  $\epsilon W_1, \epsilon L_1$ . For this reason  $W_2$  and  $L_2$  will not be numerically calculated here.

## B. EXTENSION OF THEORY TO SEAL DEVELOPMENT PROBLEM

Using the above equations and extending the mathematical development into the commonly used seal terminology, the relationship between leakage and overbalance are obtained as follows:

From 1.3 total force between sealing faces

$$W_F = \int_{r_0}^b \int_a^{2\pi} p r \cdot dr \cdot d\theta \approx W_0 + \epsilon W_1 + \epsilon^2 W_2 \quad 1.21$$

where

$$W_0 \approx .5\pi (p_b - p_a) (b^2 - a^2) \quad 1.22$$

$$W_1 \approx \frac{\mu \omega}{3h_0^2} (b-a)^3 \left[ b + a + \frac{2ab}{b+a} \right] \quad 1.23$$

$$W_2 \approx \frac{6\mu\omega}{h_0^2} \left[ -\frac{b^4 - a^4}{32} + \frac{A_1}{36} (b^3 - a^3) + \frac{B_1}{4} (b-a) + B_2 \ln \frac{b}{a} \right] \quad 1.24$$

also

$$\epsilon = \frac{\Delta h}{2 h_0} \quad 1.25$$

$$A_0 = \frac{p_b - p_a}{\ln \frac{b}{a}}$$

$$A_1 = -\frac{b^3 - a^3}{b^2 - a^2}$$

$$A_2 = -\frac{1}{2} \left( \frac{b^4 \ln b - a^4 \ln a}{b^4 - a^4} \right) - \frac{A_1}{3} \left( \frac{b^3 - a^3}{b^4 - a^4} \right) - \frac{B_1}{3} \left( \frac{b - a}{b^4 - a^4} \right)$$

$$B_1 = \frac{a^2 b^2 (b - a)}{(b^2 - a^2)}$$

$$B_2 = \frac{1}{2} \left( \frac{a^4 \ln \frac{b}{a}}{b^4 - a^4} \right)$$

From Equation 4 of Section II

$$W_F = K \pi (P_b - P_a) (b^2 - a^2) \quad 1.26$$

Combining equations 1.21, 1.22, 1.23, 1.24, 1.25, 1.26 the overbalance K can be expressed in terms of seal parameters as follows:

$$K = .5 + \frac{1.374 \times 10^{-4} \Delta h M \omega (b-a)^3}{h_o^3 (P_b - P_a) (b^2 - a^2)} \left[ b + a + \frac{2ab}{b+a} \right] + \frac{1.237 \times M \times \omega \Delta h^2}{h_o^4 (P_b - P_a) (b^2 - a^2)} \left[ \frac{b^4 - a^4}{32} - \frac{A_1}{36} (b^3 - a^3) - \frac{B_1}{4} (b-a) - B_2 \ln \frac{b}{a} \right] \quad 1.27$$

from equations 1.12 and 1.13 and 1.20 expressions for the leakage of liquid oxygen can be derived as follows:

$$Q \approx Q_0 + \epsilon Q_1 + \epsilon^2 Q_2 + \dots \quad 1.28$$

$$Q_0 \approx \frac{\pi h_o^3}{6 M} \left[ \frac{P_b - P_a}{\ln \frac{b}{a}} \right] \quad 1.29$$

$$Q_1 \approx \frac{\omega \Delta h_o}{6} \left( 2a^2 + A_1 a - \frac{B_1}{a} \right) \quad 1.30$$

$$Q_2 \approx - \frac{\omega h_o}{2} \left( \frac{a^2}{2} + a^2 \ln a + \frac{A_1}{3} a - \frac{B_1}{3a} + 2A_2 a^2 - 2 \frac{B_2}{a^2} \right) - \frac{A_o h_o^3}{4} \dots \quad 1.31$$

Assuming  $\epsilon = \frac{\Delta h}{2h_o}$

$$Q = 1.989 \times 10^5 \frac{h_o^3 (P_b - P_a)}{\mu \ln \frac{b}{a}} \quad -$$

$$1.64 \times 10^2 \omega \Delta h \left[ \frac{a^2}{2} + A_1 a - \frac{B_1}{a} \right] \quad -$$

$$1.23 \times 10^2 \omega \frac{\Delta h^2}{h_o} \left[ \frac{a^2}{2} + a^2 \ln a + \frac{A_1}{3} a - \frac{B_1}{3a} + 2A_2 a^2 - 2 \frac{B_2}{a^2} \right]$$

$$-75.79 \frac{h_o \Delta h^2 (P_b - P_a)}{\mu \ln \frac{b}{a}} \quad 1.32$$

Converting leakage of liquid oxygen at 160°F and 450 psi to

gaseous oxygen at 160°R and 15 psia results in  $Q_{gas} = Q \times 7800$  1.33

### C. APPLICATION OF THEORY TO LIQUID OXYGEN SEAL

Equation 1.27 and 1.32 are sufficient to obtain leakage Q in terms of overbalance K.

$$b = 3.45 \text{--In.}$$

$$a = 3.335 \text{--In.}$$

$$P_b = 450.0 \text{ psia}$$

$$P_a = 0 \text{ psia}$$

$$\mu = 9.17 \times 10^{-7} \text{ lb}_m/\text{in sec.}$$

$$\omega = 419 \text{ rad/sec (N = 4,000 rpm)}$$

$$\text{O.B.} = .92 \text{ (design)}$$

$$\Delta h = 400 \times 10^{-6} \text{ inches (typical from measurements before installation)}$$

The results of this calculation are shown in Figure B-2 where the leakage is plotted against overbalance for values of waviness from  $\Delta h = 500 \times 10^{-6}$ -in. to  $\Delta h = 100 \times 10^{-6}$ -in.

For the seal having .92 overbalance and waviness of  $200 \times 10^{-6}$  to  $400 \times 10^{-6}$ -in., expected leakage would be 800,000 cc/min. to 1,600,000 cc/min. as shown in Figure B-2. This compares favorably with 800,000 cc/min. actually recorded in the tests with this type of seal.

#### IV. CONCLUSIONS

A calculation of leakage from the liquid oxygen seal design parameters and the degree of "overbalance", on the basis of hydrodynamic film theory, was made. A surprisingly close agreement between the calculated and experimentally observed values of leakage was obtained.

The calculated thickness of the hydrodynamic film shown on Figure A-2 is less than the waviness of the seal surface. This can be interpreted as indicating interrupted film (carbon to ring contact at the asperities and fluid film in the surface depressions). The experimental evidence of carbon wear in presence of high leakage rate is in agreement with this interpretation.

The major deficiency of the mathematical model is that the seal surface deformation is not determined as a function of hydraulic film pressure. With highly flexible seals, like the liquid oxygen seal, it is probably the combination of film forces and carbon flexibility that determines waviness of the surface during operation and therefore the rate of leakage and wear. For the present, the only possible course was to assume that the surface waviness of the seal, as measured prior to tests and generally of the order of  $3 \times 10^{-4}$  to  $5 \times 10^{-4}$  inches was not changed substantially when the hydraulic forces were acting on both sides of the seal during running.

In addition, a single phase incompressible flow was assumed in the mathematical model and the solution was derived assuming small surface perturbations (waviness). In fact, the solution was used for calculation of leakage through large gaps and therefore further investigation and perhaps modifications and additions to the model may be required before its general usefulness to the predictions of seal performance from design parameters is established.

Specifically, it is felt that inclusion of two-phase flow, carbon flexibility, and the vibration in presence of a fluid film (or partial fluid film) between sealing surface, would bring the present model closer to describe a real seal operation.

#### REFERENCE:

1. Navahandi, A. and Osterle, F., "The Effect of Vibration on the Load Capacity of Parallel Surface Thrust Bearings", ASME Paper No. 60-LUBS-3 March 1960
2. A. Brkich, "Mechanical Seals, Theory and Criteria for Their Design" Product Engineering April 1950
3. F. A. Lyman and E. Saibel, "Leakage Through Rotary Shaft Seals" Proceedings of the fourth National Congress of Applied Mechanics 1962, Vol. 2, pp 1399 and ff.

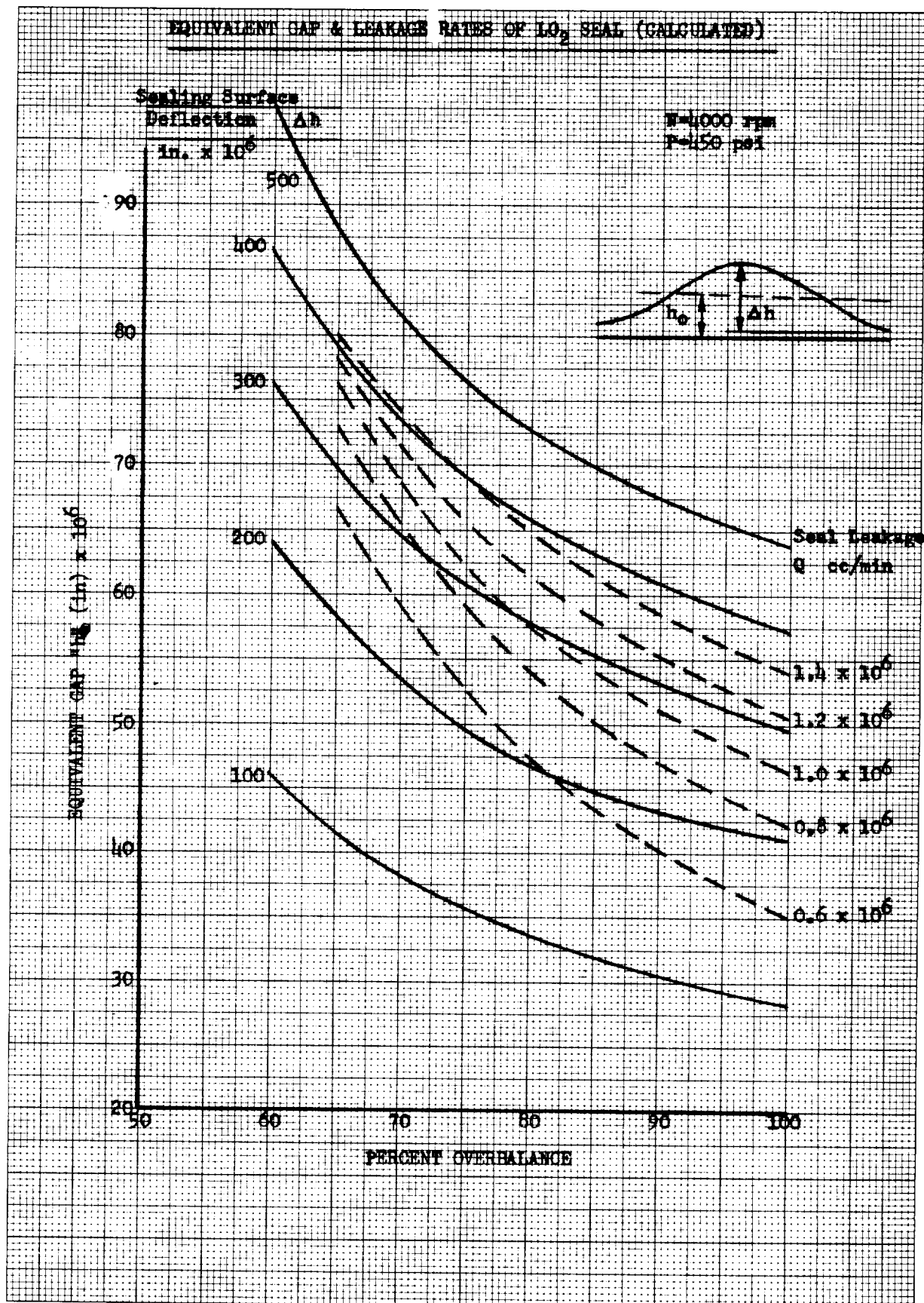


Figure B-2



REPORT NASA CR 54818 DISTRIBUTION LIST

W. F. Dankhoff (3 Copies)  
NASA  
Lewis Research Center  
21000 Brookpark Road  
Cleveland, Ohio 44135  
Mail Stop 500-305

J. A. Durica (1 Copy)  
Mail Stop 500-210

Patent Counsel (1 Copy)  
Mail Stop 77-1

Lewis Library (2 Copies)  
Mail Stop 3-7

Lewis Technical Information  
Division (1 Copy)  
Mail Stop 5-5

H. J. Hartmann (1 Copy)  
Mail Stop 5-9

J. C. Montgomery (1 Copy)  
Mail Stop 501-1

Major E. H. Karelis (1 Copy)  
Mail Stop 4-1

Lewis Office of Reliability  
and Quality Assurance (1 Copy)  
Mail Stop 500-203

R. L. Johnson (1 Copy)  
Mail Stop 5-8

F. J. Dutee (1 Copy)  
Mail Stop 23-1

NASA Headquarters (6 Copies)  
Technical Information Abstracting  
and Dissemination Facility  
Box 5700  
Bethesda, Maryland

Library (1 Copy)  
NASA  
Ames Research Center  
Moffett Field, California 94035

Library (1 Copy)  
NASA  
Flight Research Center  
P. O. Box 273  
Edwards AFB, California 93523

Library (1 Copy)  
NASA  
Goddard Space Flight Center  
Greenbelt, Maryland 20771

Library (1 Copy)  
NASA  
Langley Research Center  
Langley Station  
Hampton, Virginia 23365

Library (1 Copy)  
NASA  
Manned Spacecraft Center  
Houston, Texas 77058

Library (1 Copy)  
NASA  
George C. Marshall Space Flight Center  
Huntsville, Alabama 35812

Library (1 Copy)  
NASA  
Western Operations Office  
150 Pico Boulevard  
Santa Monica, California 90406

Library (1 Copy)  
Jet Propulsion Laboratory  
4800 Oak Grove Drive  
Pasadena, California 91103

A. C. Tischler (2 Copies)  
NASA Headquarters  
Code RP  
Washington, D. C. 20546

J. W. Thomas, Jr. (5 Copies)  
NASA  
George C. Marshall Space Flight Center  
Code I-E-E, Huntsville, Alabama 35812

E. W. Gomersall (1 Copy)  
NASA  
Mission Analysis Division  
Office of Advanced Research and Technology  
Moffett Field, California 94035

Dr. E. B. Konecni (1 Copy)  
National Aeronautics and Space Council  
Executive Office of the President  
Executive Office Building  
Washington, D. C.

H. V. Main (1 Copy)  
Air Force Rocket Propulsion Laboratory  
Edwards Air Force Base  
Edwards, California

F. Iura (1 Copy)  
Aerospace Corporation  
2400 East El Segundo Blvd.  
P. O. Box 95085  
Los Angeles, California 90045

F. Chahmemani (1 Copy)  
Aerospace Corporation  
2400 East El Segundo Blvd.  
P. O. Box 95085  
Los Angeles, California 90045

Pratt and Whitney Aircraft Corporation (1 Copy)  
Florida Research and Development Center  
P. O. Box 2691  
West Palm Beach, Florida 33402

Rocketdyne (1 Copy)  
Division of North American Aviation  
Library Department 586-306  
6633 Canoga Avenue  
Canoga Park, California 91304

Justus Stevens (1 Copy)  
Sealol Company  
P. O. Box 2158  
Providence 5, Rhode Island

